Doctoral Thesis

DESIGNING MPC-BASED AGC SCHEMES CONSIDERING GENERATOR DYNAMIC MODELS

발전기 동적 특성을 고려한 MPC 기반 AGC 전략 설계

August 2015

Graduate School of Seoul National University

Department of Electrical Engineering and Computer Science

Young-Sik Jang

DESIGNING MPC-BASED AGC SCHEMES CONSIDERING GENERATOR DYNAMIC MODELS

발전기 동적 특성을 고려한 MPC 기반 AGC 전략 설계

Young-Sik Jang

Submitting a doctoral thesis of Electrical Engineering

June 2015

Graduate School of Seoul National University

Department of Electrical Engineering and Computer Science

Yong Tae Yoon

Confirming the doctoral thesis written by Young-Sik Jang

June 2015

Chair 박종근 **(Seal)**

Vice Chair 윤용태 **(Seal)**

Examiner 문승일 **(Seal)**

Examiner 김건중 **(Seal)**

Examiner 최재석 **(Seal)**

ABSTRACT

DESIGNING MPC-BASED AGC SCHEMES CONSIDERING GENERATOR DYNAMICS MODELS

Young-Sik Jang

Department of Electrical Engineering and Computer Science

Seoul National University

This thesis proposes a novel model predictive control (MPC)-based approach for automatic generation control (AGC) to reduce problems, such as decreasing dynamic performances of AGC and control instability, which result from constraints in load-reference set-point ramp rate and delayed inputs of generators. In general, traditional proportional–integral (PI)-based approach for AGC is unmanageable, and dealing with the problems is difficult because the approach is a single-input-single-output (SISO) control model. Moreover, the problems gradually increase via the traditional PI-based approach, whereas power systems grow. Therefore, this thesis proposes and develops the MPC-based approach for AGC schemes.

First, this thesis proposes a discretized control process design in a continuous network-generator dynamics model, referring to two earlier PhD theses conducted on this topic at Massachusetts Institute of Technology in the United States. As a real system, the given continuous network-generator dynamics model shows that the frequencies among generators in a balancing area can be different. This situation indicates that the system frequency used to compute area control error is a representative frequency in its area. Given

that the discrete-time state feedback control signals (i.e., the load reference set points) are periodically transmitted to generators for every sampling time, this thesis proposes a process design to control multiple generators through the generator frequencies rather than a representative frequency and uses multiple time scales because the control process is activated in a discrete-time manner.

Second, this thesis proposes a controller considering the delayed inputs of generators. Using MPC-based approach, this thesis first develops a conversion process for the delayed-input system models to create a delay-free system model. Based on the obtained model, this thesis proposes a controller that considers the generator characteristics using a quadratic cost criterion, which is a squared-weighted sum of states (regulated variables: generator frequencies) and controls (load reference set point) among multiple generators. Specifically, quadratic programming algorithm is adopted to reduce computing time and cost.

Finally, this thesis proposes a novel bulk-area partitioning scheme to reduce computation cost. Although simple modified SISO-based schemes, such as PI-based AGC, do not suffer greatly from this problem, the number of generators in a bulk area leads to computational burden via the proposed controller. According to the number of participating generators in AGC, computation times to calculate the AGC signal are compared, and this thesis proposes the bulk-area partitioning scheme in accordance with the results to reduce computation time and ensure dynamic performance.

Both traditional PI-based and proposed MPC-based AGCs are simulated in four conditions based on the constraints of load reference ramp and input time delays. For quantitative analysis, this thesis shows that the frequency settling time, the quantity of inadvertent tie-line flows, and CPS are analyzed by comparing them with the traditional PI-based approach. Moreover, the MPC-based operation results are also analyzed from the perspective of computational cost.

KEYWORDS:

Automatic generation control (AGC), Model predictive control (MPC), Multiple-inputs multiple-outputs (MIMO) system, Power network, Time-delay

STUDENT NUMBER: 2009-20885

CONTENT

List of Figures

List of Tables

CHAPTER 1. INTRODUCTION

1.1 IMPETUS FOR THE THESIS

Bulk power systems are usually composed of interconnected balancing areas (BAs) to minimize the operation cost from arbitrage trading and to increase the system reliability by importing electric power. Each BA has its own automatic generation control (AGC) scheme in energy management system (EMS), which is responsible for maintaining a nominal frequency and stabilizing inadvertent tie-line flows to scheduled flows. AGC signals are traditionally developed to minimize area control errors (ACEs), which represent the discrepancy between generation supply and total megawatt (MW) obligation in each BA [1].

Conventionally, AGC signals from EMSs are transmitted via dedicated communication channels. In natural dynamic processes, input time delays are often encountered in transmitting information among different parts of a system because of the response speed of each part [2, 3]. Therefore, the AGC system is an example of a time-delayed system because it uses communication channels under a hierarchical control structure, and has various generation units with different power-output response times to the AGC signal. Figure 1.1 shows the description of load-reference set-point reaction to a given AGC signal at time T_u in a single generator.

In the field, time-delayed systems frequently encounter control instabilities that lead to performance degradation. For this reason, time-delayed systems have attracted significant interest, and several reports on power systems have addressed AGC modeling/synthesis in the presence of delays in the input signals [4-9].

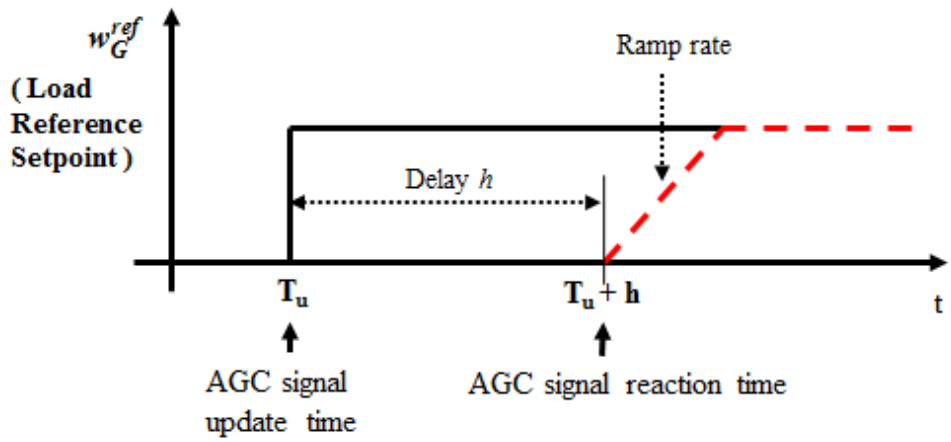

Figure 1. 1 Load reference set-point update description in a single generator

Ayasun [4] and Jiang [5] investigated the effects of time delays on stability. They showed that a delay significantly decreased the admissible controller gain in proportional–integral (PI) AGC or made the AGC system less stable. Bhowmik [6] demonstrated the need to include the effects of communication delays in frequency regulation, and discussed the requirements of communication networks. Sasaki [7] showed that the control performance standard (CPS) decreased as the time delay increased. Hassan [8, 9] proposed a new PI-based controller design for time-delayed power systems. These studies mainly described the economic and systemic concerns of time-delayed input signals via PI-based approaches.

Although these studies dealt with maintaining the time-delayed system, the AGC signal was computed considering a single generator. The characteristics of multiple generators should be considered, however, because the constraints of load-reference ramp rate and power-output response times vary among generators and have a significant effect on the overall dynamic performance, such as the CPS and settling times for the frequency. For example, to rapidly stabilize frequency deviations and inadvertent tie-line flows among BAs, shorter response times of generators are desirable. Therefore, generators with slow

response time or under constrained conditions should be sublated when AGC signals are computed by the EMS in each BA.

Moreover, providing an effective method to reduce the problems caused by delayed inputs among generators is difficult for the traditional PI-approach because it is a SISO-based scheme that cannot consider the future implications of current control action. Specifically, when inputs among multiple generators are delayed, the future states (frequencies) should be considered on the basis of previous inputs (load-reference set point) because excessive control inputs without considering previous inputs may result in control instability [4, 5].

1.2 OBJECTIVES OF THE THESIS

This thesis designs and develops a novel MPC-based approach for AGC to improve the control performance. This thesis mainly deals with delayed inputs and load reference (set point) ramp rates among generators. In general, the traditional PI-based approach for AGC is unmanageable, and dealing with these characteristics among generators is difficult because the approach is a SISO-based control model. The problems that result from delayed inputs gradually increase, whereas power systems grow. Therefore, a new model for AGC is proposed.

Based on the proposed model, the objectives of this thesis address three main questions.

The first question is how to determine the discrepancy between generation supply and total megawatt (MW) obligation in each BA when delayed inputs exist among generators. Answering this question is the most important objective in this thesis. Considering delayed inputs, this thesis mainly develops the process to convert the delayed-input system models into an equivalent delay-free system model. Based on this process, this thesis shows that the previous control inputs should be reflected while the controller computes the discrepancy.

The second question is which generator can be valuable and useful in satisfying the primary objectives of AGC, such as stabilizing frequency and maintaining the scheduled tie-line flows. This thesis shows that shorter response times among generators are better. Another important question is how to allocate the generation resources at each AGC signal when generators have constraints in load-reference (set-point) ramp rates. In this case, an optimization process should be developed to reflect the characteristics of generators. Therefore, quadratic programming algorithm is adopted to effectively allocate the generator resources based on their characteristics and to reduce the computational cost as a result of algorithm complexity.

The third question is what are the major drawbacks of the MPC-based approach and how to minimize them. Although simple modified SISO-based schemes, such as PI-based AGC, did not suffer greatly from the computational cost to calculate AGC signals every sampling time, the proposed controller significantly suffers from the computational cost because the number of generators in bulk areas leads to a “curse of dimensionality” in the optimization process. According to the number of participating generators in AGC, computation times to calculate AGC signal are compared via the proposed approach. This thesis proposes a novel bulk-area partitioning scheme consistent with the results to reduce computation time and ensure dynamic performance.

1.3 THESIS ORGANIZATION

The remainder of this thesis is organized into several chapters.

Chapter 2 introduces the background of the basic system model to develop the proposed controller. First, network-generator dynamics coupling model is adopted. This model is the continuous dynamics model presented in two earlier PhD theses conducted on this topic at MIT [10, 11]. Based on the continuous model, this thesis develops a discretized multi-input-multi-output (MIMO) controller for AGC. Second, we introduce the primary objectives of AGC and the traditional PI-based approach for AGC. In this part, we mainly show how the description of the traditional PI-based approach for AGC is developed to satisfy the primary objectives of AGC, and the previous research on delayed inputs is analyzed. Finally, we introduce the basic principle of the MPC-based approach, and the previous research on this approach for AGC is examined. The proposed MPC-based model significantly differs from the previous research because the proposed model mainly considers multiple machines in BA rather than a single machine.

Chapter 3 presents the mathematical formation of the MPC-based approach for AGC and analyzes the difference between traditional PI-based approach and MPC-based approach. First, Chapter 3 discusses the proposed MPC-based approach for AGC. Considering the spatial structures, both single- and multi-area cases are developed. Moreover, this section mainly provides the process to convert the delayed-input system models into a delay-free system model, and develops the controller based on a quadratic cost criterion, which is a squared-weighted sum of states (regulated variables: generator frequencies) and controls (load-reference set point) among multiple generators. Second, this chapter provides the bulk-area partitioning schemes to reduce the computational burden, which is one of major drawbacks of the MPC-based approach. For instance, the number of generators in bulk areas result in computational burden, although simple modified SISO-

based schemes, such as the conventional PI-based AGC, do not suffer greatly from this problem. Finally, both traditional PI-based and MPC-based approaches are analyzed from the perspective of control structure.

Chapter 4 presents the illustrative examples. First, based on a unit-step disturbance, both approaches are simulated in four scenarios through load-reference ramp constraints and input time delays. For quantitative analysis, this thesis shows that the frequency settling time and the quantity of inadvertent tie-line flows are analyzed by comparing them with the traditional PI-based approach. Second, this chapter also shows the simulation results based on the continuous load model, which is developed by stochastic Ornstein–Uhlenbeck process. In this section, we investigate and analyze the results of the frequency control system for approximately 4 h to analyze the CPS results using both approaches. Finally, this chapter shows that the number of generators or a large prediction horizon size significantly increases the computation time. Therefore, we also show that the proposed bulk-area partitioning scheme effectively reduces the computational cost and provides only a slight difference in dynamic performance compared with the original case result in the distributed structure.

Chapter 5 concludes the study and presents the future research directions pertinent to the presented work.

We provide a control model in the Appendix to enhance another advantage of the MPC-based approach and introduce the description of CPS to help the reviewers understand the simulation results in the continuous load case. Specifically, the individual line-flow control model is provided to reduce the wheeling in the power network. As loop flows and arrangements for parallel path compensation become increasingly important, this developed control scheme supports the system operators by reducing the increase in power losses or the overloading of network elements.

CHAPTER 2. BASIC SYSTEMS MODEL

2.1 GENERATOR AND POWER NETWORK DYNAMICS

This section presents the network-generator dynamics coupling model, which is adopted in this thesis. Based on this model, this thesis develops a Multi-Inputs-Multi-Outputs controller for AGC.

2.1.1 NETWORK DYNAMICS MODEL

By linearizing power network equations under the decoupling assumption (i.e., $\partial P^N / \partial V = 0$), we obtain Eq. (2.1) [12] given by

$$P^N = \begin{bmatrix} P_G + F_G \\ -P_L + F_L \end{bmatrix} = \begin{bmatrix} J_{GG} & J_{GL} \\ J_{LG} & J_{LL} \end{bmatrix} \begin{bmatrix} \delta_G \\ \delta_L \end{bmatrix} \tag{2.1}$$

Where

$$J_{ij} = \frac{\partial P_i^N}{\partial \delta_j}, \qquad i, j \in \{G, L\}$$

G and L represent a set of all generators and loads in the area, respectively. F_G and F_L are the injected powers, such as tie-line flows, uncontrollable power source outputs, and/or the load demands at generator bus. From Eq. (2.1), we obtain Eqs. (2.2) and (2.3) given by

$$\begin{aligned} P_G &= (J_{GG} - J_{GL}J_{LL}^{-1}J_{LG})\delta_G + J_{GL}J_{LL}^{-1}P_L + J_{GL}J_{LL}^{-1}F_L - F_G \\ &= K_P\delta_G + D_P P_L - F \end{aligned} \tag{2.2}$$

$$\dot{P}_G = K_P\dot{\delta}_G + D_P\dot{P}_L - \dot{F} \tag{2.3}$$

The network model in Eq. (2.3) shows that the power output of the system generators is affected by disturbances (P_L and F) and generator angle (δ_G). In Eq. (2.3), $\dot{\delta}_G$ is the generator frequency w_G.

2.1.2 GENERATOR DYNAMICS MODEL

Figure 2.1 shows the control loop of a single generator in a network topology. (In this part, the symbol Δ, representing a change of state between two before and after, was omitted for a concise expression.)

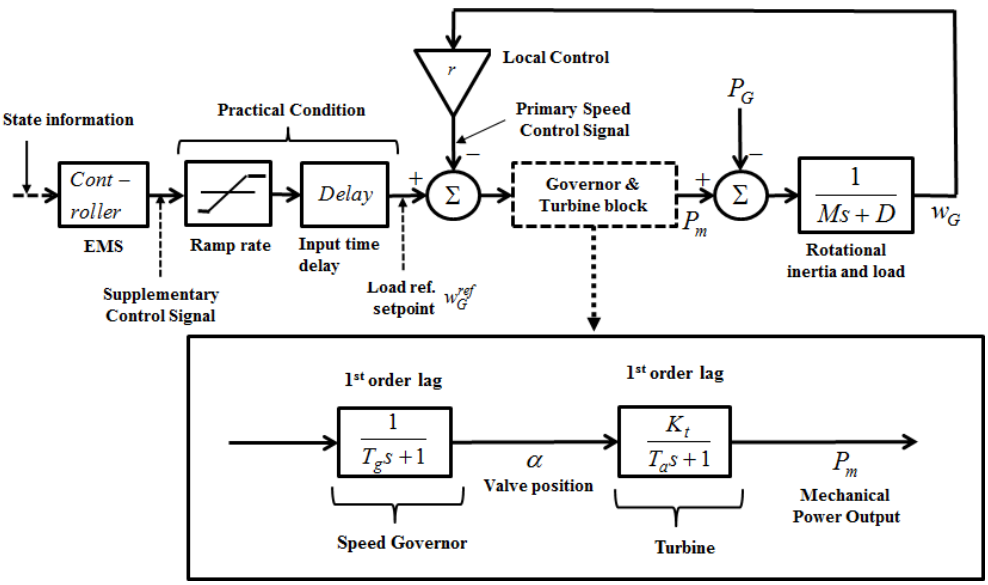

Figure 2. 1 Primary control loop of a G-T-G set

Based on Figure 2.1, an electric generator is represented by a continuous-time model, such as that given in Eq. (2.4) [10, 11]. This model represents the characteristics of a drooping governor and discretized frequency control. The discrete-time state feedback control w_G^{ref}, which is the load reference (set-point) through AGC, is periodically updated for every sampling time, T_u. In this case, we consider T_f in order to obtain more accurate control signal based on delayed-inputs because delayed-inputs could occur between load reference update signals.

$$\begin{bmatrix} \dot{w}_G \\ \dot{P}_m \\ \dot{\alpha} \end{bmatrix} = \begin{bmatrix} -\frac{D}{M} & \frac{1}{M} & 0 \\ 0 & -\frac{1}{T_a} & \frac{K_t}{T_a} \\ -\frac{1}{T_g} & 0 & -\frac{r}{T_g} \end{bmatrix} \begin{bmatrix} w_G \\ P_m \\ \alpha \end{bmatrix} + \begin{bmatrix} -\frac{1}{M} \\ 0 \\ 0 \end{bmatrix} P_G + \begin{bmatrix} 0 \\ 0 \\ \frac{1}{T_g} \end{bmatrix} w_G^{ref}(t-h) \quad (2.4)$$
$$= \mathrm{A}_{pri} z + B w_G^{ref}(t-h) + C P_G$$

where

$$w_G^{ref}(t\text{ - }h) = w_G^{ref}(k_u T_u - h) + u(k_u T_u - h)(t - k_u T_u)\,, \quad k_u T_u \le \mathrm{t} \le (k_u + 1)T_u$$

In Eq. (2.4), P_G is the real (electrical) power output supplied by the generator. However, P_G is no longer an independent input when generators are connected together because P_G depends on constraints imposed by interconnections with other generators, loads (P_L), and tie-line power flows (P_f) from neighboring areas [10, 11].

For this machine model in Eq. (2.4), a steady-state solution for w_G can be found solely in terms of P_G, the network constraint, and w_G^{ref}, the load reference control. The steady-state solution is given in [12] as:

$$w_G[k] = (1 - \sigma D) w_G^{ref}[k-h] - \sigma P_G[k] \quad (2.5)$$

where

$$\sigma = \frac{r}{rD + K_t}$$

An equivalent definition for the droop constant σ is

$$\sigma = -\left.\frac{\partial w_G[k]}{\partial P_G[k]}\right|_{w_G^{ref}[k-h]=0} \quad (2.7)$$

2.1.3 GENERATOR AND NETWORK COUPLING MODEL

From Eqs. (2.3) and (2.4), the extended-state space (or full-scale dynamics model) can be expressed as [11, 12]

$$\begin{bmatrix} \dot{\bar{z}} \\ \dot{\bar{P}}_G \end{bmatrix} = \begin{bmatrix} A_{pri}^{bd} & C^{bd} \\ K_p e^{bd} & 0 \end{bmatrix} \begin{bmatrix} \bar{z} \\ \bar{P}_G \end{bmatrix} + \begin{bmatrix} B^{bd} \\ 0 \end{bmatrix} \bar{w}_G^{ref}(t-h) + \begin{bmatrix} 0 & 0 \\ -I & D_p \end{bmatrix} \begin{bmatrix} \dot{F} \\ \dot{P}_L \end{bmatrix} \tag{2.8}$$

where $\bar{z}$ and $\bar{P}_G$ describe concatenation representations of machine state spaces and the electric power output of generators; $\bar{w}_G^{ref}$ is a concatenation representation of load reference setting, e = [1 0 0]; and the matrices with superscript *bd* show block diagonal matrices with each matrix (e.g., A_{pri}^{bd}= diag [A_{pri}^{1},.. A_{pri}^{i},.. A_{pri}^{n}], where the number i indicates each generator). As shown in Figure 2.2, multiple frequencies can be considered in transient state, and the model in eq. (2.8) describes this phenomenon.

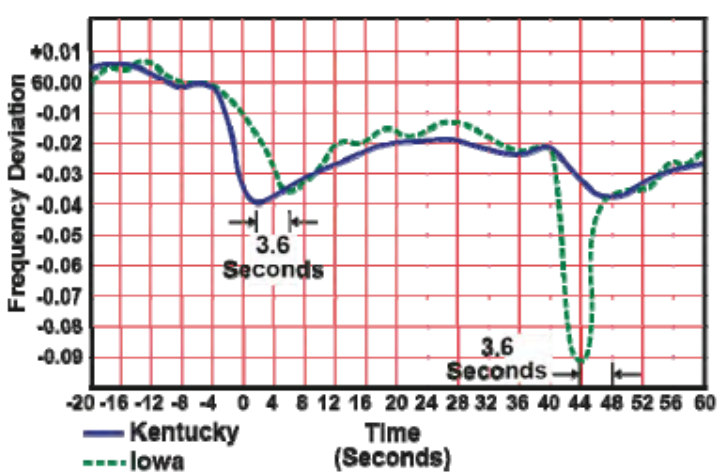

Figure 2. 2 Speed of the traveling frequency waves [1]

From a structural point of view, the electric power output of generators, P_G, is a natural choice for state variables. This set of state can be interpreted in terms of the interaction of the generators with the transmission system.

From Eqs. (2.2) and (2.5), the discretized causal model with the *n*-generator frequency sampling time T_f can be expressed as [11]

$$\begin{aligned} w_G[k+1] &= (\mathrm{I}+\mathrm{K}_p\,\Omega\,\mathrm{T}_f)^{-1}\{w_G[k]+(\mathrm{I}-\Omega\Phi)u[k-h] \\ &\qquad +\Omega(f[k]-D_P d[k])\} \\ &= Aw_G[k]+Bu[k-h]+d_w[k] \end{aligned} \tag{2.9}$$

where

$$\Omega = \mathrm{diag}\,[\sigma_1, \sigma_2, \ldots \sigma_n]$$

$$\Phi = \mathrm{diag}\,[D_1, D_2, \ldots D_n]$$

$$u[k-h] = w_G^{ref}[k+1-h] - w_G^{ref}[k-h]$$

$$f[k] = F[k+1] - F[k]$$

$$d[k] = P_L[k+1] - P_L[k].$$

As a discrete-time process, w_G in Eq. (2.9) is not perfectly matched with the initial (transient) behavior of w_G in Eq. (2.8), but it captures slower frequency dynamics reasonably well [11].

2.2 PI-BASED APPROACH FOR AGC

This section introduces background of traditional AGC in power system. Especially, we mainly show how traditional PI-based approach for AGC is developed in order to satisfy the primary objectives of AGC, and the previous researches on delayed-inputs are analyzed.

2.2.1 PRIMARY OBJECTIVES OF AGC

In any electric system, the active power has to be generated as it is consumed at the same time, and the generated power must be maintained in constant equilibrium with power consumed/demanded. Disturbances in this balance cause a deviation of the system frequency from its nominal values since they are offset initially by the kinetic energy of the rotating generating sets and motors connected [13]. Because constancy of speed of motor drives is particularly important for satisfactory performance and stable operation of generating units, the frequency must be maintained within strict limits [1, 14].

AGC is one of means to balance the active power. The primary objectives of AGC are to regulate frequency to the specified nominal value and to maintain the interchange power between control areas at the scheduled values by adjusting the output of selected generators. This function is commonly referred to as load-frequency control (LFC). Based on this function, discrepancy between generation supply and total megawatt (MW) obligation in each BA are reduced. A secondary objective is to distribute the required change in generation among units to minimize operating costs through using participation rates of each unit [14].

In the field, most real-world AGC systems use PI-based controller, and the controller's output signal is developed to minimize area control errors (ACEs), which represent the discrepancy between generation supply and total megawatt (MW) obligation in each BA

[1]. Based on the control outputs, the load reference set-points of the participating generators in AGC are changed by the participation rate of each unit.

2.2.2 PI-BASED APPROACH

2.2.2.1 INTRODUCTION [15, 16]

Proportional–Integral (PI) controller has a long history in the automatic control field, starting from the beginning of the last century. Owing to its intuitiveness and its relative simplicity, in addition to satisfactory performance which it is able to provide with a wide range of processes, it has become in practice the standard controller in industrial settings.

In control designing, applying a PI-based control law consists of applying properly the sum of two types of control actions: a proportional action and an integral action. These actions are described as below.

- Proportional Action

The proportional control action is proportional to the current control error, according to the expression

$$\begin{aligned} u(t) &= K_p e(t) \\ &= K_p (y(t) - r(t)) \end{aligned} \tag{2.10}$$

where K_p is the proportional gain, $r(t)$ is a nominal set-point value and $y(t)$ is a measured value. Its meaning is straightforward, since it implements the typical operation of increasing the control variable when the instantaneous error, $e(t)$, is large (with appropriate sign). The Laplace transfer function of a proportional controller can be derived trivially as

$$C(s) = K_p \tag{2.11}$$

The main drawback of using a pure proportional controller is that it produces a steady-state error. It is worth noting that this occurs even if the process presents an integrating dynamics, in case a constant load disturbance occurs.

- Integral Action

The integral action is proportional to the integral of the control error, i.e., it is

$$u(t) = K_i \int_0^t e(\tau) d\tau \tag{2.12}$$

where K_i is the integral gain. It appears that the integral action is related to the past values of the control error. The corresponding transfer function is:

$$C(s) = \frac{K_i}{s} \tag{2.13}$$

In other words, the integral action is able to automatically reduce steady-state error caused via a pure proportional controller. Thus, the use of a proportional action in conjunction to an integral action, i.e., of a PI controller, solves the main problems of the oscillatory response associated to an On–Off controller and of the steady-state error associated to a pure proportional controller. Figure 2.3 shows the block diagram of PI-based controller.

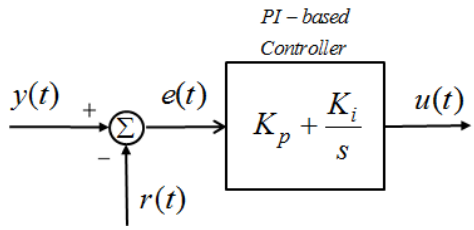

Figure 2. 3 Block diagram of a PI-based controller [16]

2.2.2.2 PI-BASED APPROACH FOR AGC

As mentioned before, the basic objective of AGC is to restore balance between each area load and generation. This is met when the control action maintains

- Frequency at the scheduled value
- Net interchange power with neighboring areas at scheduled values.

According to these objectives, most of real-world AGC systems uses PI-based controllers, and control output signals are developed to minimize area control errors (ACEs), which can be described as

$$\begin{aligned} ACE_i &= P_{i,f}^{net} - 10\mathrm{B}\cdot w_{i,G}^{rep} \\ &= P_{i,f}^{net} + \beta\, w_{i,G}^{rep} \end{aligned} \tag{2.14}$$

where the subscript i, representing i-BA, $P_{i,f}^{net}$ is the deviated net interchange [MW], which is computed by the actual net interchange minus the scheduled net interchange, B is the frequency bias factor [MW / Hz], and $w_{i,G}^{rep}$ is the deviated system frequency, which is computed by the actual system frequency minus the scheduled (nominal) system frequency.

This situation signifies that ACE_i in Eq. (2.14) is the state information in Figure 2.1 and the instantaneous error $e(t)$ in Figure 2.3.

ACE_i is a very implicative information about a given system i. Especially, the system frequency is required to be accurately measured and properly selected since there are different frequencies among generators as shown in Eq. (2.8) and Figure 2.2. Moreover, the frequency bias factor B should be carefully tuned since it varies according to the generators' operating points [17, 18].

Figure 2.4 shows the control loop of the conventional PI-based approach for AGC when there are multiple-generators. It used a single input, which is the present state error (ACE), and a single output was computed by considering the present state error. Therefore, it is mainly required to obtain the accurate ACE and to tune the gain parameters in order to improve the dynamic performance of AGC.

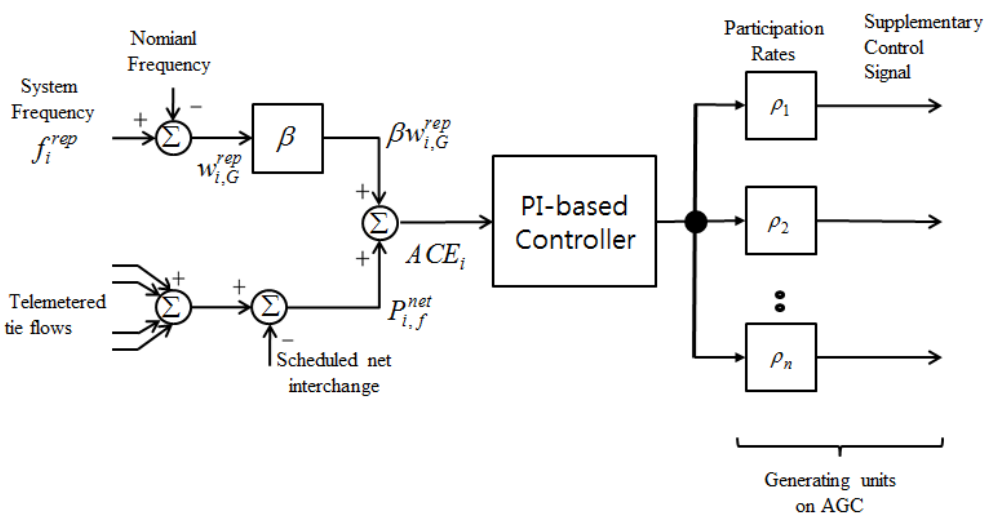

Figure 2. 4 Block diagram of PI-based approach for AGC considering multiple-generators [9, 14]

2.2.2.3 LIMITATIONS OF PI-BASED APPROACH FOR AGC

As shown in Figures 2.3 and 2.4, PI-based controller is mainly designed for the SISO control system. Therefore, in the conventional AGC, it was required to accurately compute the ACE considering multiple inputs, which are the deviated generators' frequencies and the inadvertent tie-line flows, and to properly tune the gain parameters in order to improve the control performance.

PI-based approach has a severe limitation to deal with delayed inputs among generators. When there are the delayed inputs among multiple generators, the future states (frequencies) should be considered based on the previous inputs (load reference set-point) because the excessive control inputs without considering previous inputs cause control instability. In general, PI-based approach is not able to consider the future implication of current control action since it is a SISO-based controller. Therefore, previous researches [4-9] showed that a delayed input based on a single generator significantly decreased the admissible controller gain in PI-based AGC, or made the AGC system less stable. Moreover, to improve the control stability, choosing a small integral gain in PI-based approach can cause poor dynamic performance of AGC. The details of the integral gains in PI-based approach are simulated and discussed in Chapter 4.

PI-based approach is difficult to do on-line constraint handling in a systemic way. In the field, the participating generators in AGC are different load reference set-point ramp rates. Therefore, it is necessary to solve the optimization problem subject to constraint satisfaction. However, conventional AGC used a single input, which is the present state error (ACE), and a single output was computed by considering the present state error only. Since the output (control signal) was optimized (computed) and transmitted through fixed constant participation rates among generators without taking explicit account of the constraints among generators, the dynamic performance was actually poor under

constrained conditions. The details of the constraints among generators in PI-based approach are simulated and discussed in Chapter 4.

In summary, PI-based approach is not an effective method to solve the resource allocation problems in MIMO systems even though simple SISO-based approach can be easily realized [19]. As shown in Figure 2.4, each generator in AGC is assigned with the supplementary control signals, which are the load reference set-point changes. Without loss of generality, this signals should be computed based on the characteristics of multiple generators since generators with a slow response time or under constrained conditions should be sublated. However, the practical resource allocation process is realized via constant participation rates [14]. Therefore, it is additionally required to develop the resource allocation algorithm to exploit the characteristics of multiple-generators.

2.3 MODEL PREDICTIVE CONTROL

This section introduces the basic principle of MPC-based approach, and the previous researches of MPC-based approach for AGC are analyzed.

2.3.1 INTRODUCTION

A system is assumed to incorporate the state transition function and constraints in Eqs. (2.15) and (2.16) to (2.18), respectively.

$$x_{k+1} = Ax_k + Bu_k \tag{2.15}$$

subject to

$$x^{\max} \le x_k \le x^{\min} \tag{2.16}$$

$$u^{\max} \le u_k \le u^{\min} \tag{2.17}$$

$$Cx_k = l_k \tag{2.18}$$

Equation (2.15) is converted into a standard form via the model predictive control, and the following matrices are introduced.

$$\begin{aligned} X_k &= \begin{bmatrix} A \\ A^2 \\ \vdots \\ A^{hp} \end{bmatrix} x_k + \begin{bmatrix} B & 0 & \cdots 0 \\ AB & B & \cdots 0 \\ \vdots & \vdots & \ddots \vdots \\ A^{hp-1}B & A^{hp-2}B & \cdots B \end{bmatrix} \begin{bmatrix} u_{k|k} \\ u_{k+1|k} \\ \vdots \\ u_{k-1+hp|k} \end{bmatrix} \\ &= M_x x_k + C_u U_k \end{aligned} \tag{2.19}$$

where

$$X_k = [x_{k+1}|_k,\ x_{k+2}|_k,\ \ldots,\ x_{k+hp}|_k]^T$$

In Eq. (2.19), *hp* is the predictive horizon size. The advantage of Eq. (2.19) is its capacity to convert the state constraints into the control constraints of U_k. Meanwhile, Eqs. (2.16) and (2.18) are converted into the below constraint formats.

$$\begin{bmatrix} I \\ -I \\ -C_u \\ C_u \end{bmatrix} U_k \leq \begin{bmatrix} \bar{U} \\ \underline{U} \\ -X^{\min} + M_x x_k \\ X^{\max} - M_x x_k \end{bmatrix} \tag{2.20}$$

$$C_{blk} C_u U_k = L - C_{blk} M_x x_k \tag{2.21}$$

where C_{blk} is the block diagonal matrix with C, L is N-by-*1* vector with l_k for $k = 1,\ldots hp$, I is the *hp*-by-*hp* identity matrix, and $\bar{U}$ ($\underline{U}$) is the *hp*-by-*1* vector with the element $u^{\max}$($u_{\min}$).

With Eqs. (2.19), (2.20), and (2.21), MPC is utilized in such a manner that an open loop optimal control problem for any current state (i.e., a given initial state) x_k at time k is solved over some future interval with the consideration of current and future constraints. During the given period *hp*, the first value $u_k|_k$ from this optimal sequence U_k is injected into the plant as the optimal control.

The methodology of all the controllers belonging to the MPC family is characterized by the following strategy, represented in Figure 2.5. The model block is used to predict the future plant outputs X_k, based on past and current values x_k and on the proposed optimal future control actions U_k. These actions are calculated by the optimizer taking into account the cost function as well as the constraints. Specifically, the set of future inputs is calculated by optimizing a determined criteria, which is the customized objective function, in order to keep the process as close as possible to the reference trajectory.

A major difference between the MPC-based and PI-based approaches is that control designers may select the essential information from the available data in the system based on the objective and constraints, and design the controller to satisfy the system requirements. Therefore, the model block in Figure 2.5 is very important to exploit the merits of the method, in contrast to PI-based approaches. Specifically, when there are the delayed inputs among multiple generators, the future states should be considered based on the previous inputs because the excessive control inputs without considering previous inputs cause control instability. In this case, the model block can help system operators prevent excessive control inputs with considering the future state errors.

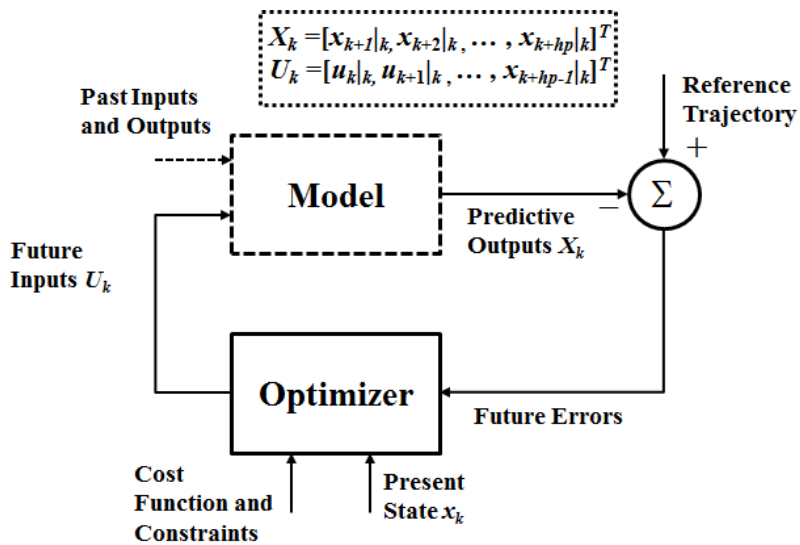

Figure 2. 5 Basic structure of MPC [19]

2.3.2 PREVIOUS RESEARCHES AND LIMITATIONS

Recently, model predictive control (MPC)-based designing process in AGC was extensively studied because of its two major advantages [19]. First, this approach provides satisfactory control performance under dynamic constraints, such as load reference ramp constraints. Second, it allows systematic design of multi-input-multi-output (MIMO) systems. The conventional PI-based approach in AGC presents intractable subjects for admissible load reference control in real-time operation. By contrast, the MPC-based approach does not suffer from these problems because the actual control objectives and operating constraints can be represented explicitly in a single multi-horizon optimization.

Several MPC-based studies and formulations are available in literature, and these approaches can be classified into three main categories, namely, centralized (single-area), distributed (multi-area), and decentralized (multi-entities) control structures.

Mohamed [20] investigated robust load frequency control (LFC) against parameter uncertainties and load changes but only dealt with LFC control application in a single-area power system. Kong [21] proposed state contractive constraint-based MPC algorithms to guarantee the stability of the control scheme. Yousef [22] utilized the MPC technique to investigate the design of the LFC system and thus improve power system dynamic performance over a wide range of operating conditions. However, centralized MPC-based AGC [20-22] among independent bulk BAs is stated to be an impractical approach [23, 24] because each BA should have its own AGC scheme, and optimizing AGC signals in a large-scale power system model consumes the computational time to obtain an admissible solution.

Camponogara [23] introduced the coordination of optimization computations using iterative exchange of information among distributed BAs. Venkat [24] proposed a new object function that measures the system-wide effect of local control actions to build a

reliable MPC-based controller. Nong [25] provided a distributed MPC with fuzzy modeling to deal with the valve limit on the governor. Ma [26] provided an MPC-based AGC that considers generation rate constraint and load reference ramp constraint. However, these distributed studies [23-26] assumed that the dynamic model in each area is modeled as a single-input-single-output (SISO) model, even when each BA has various local frequencies and multiple generators as the MIMO system [1]. Control signals in each BA should also be periodically updated because EMS is a discretized controller [14].

A few of the decentralized approaches are introduced or briefly mentioned in literature [24, 27]. However, these control schemes are necessary to build a highly reliable and real-time communication system because each entity should communicate with other entities in real time to minimize the system-wide effects of local control actions and maximize its profits.

Even though the previous researches dealt with modeling issues of AGC, there were the critical two limitations in the researches [20-27].

First, they mainly dealt with a single generator model rather than multiple-generators in AGC. Therefore, the previous models have the same drawbacks of PI-based approach while there are multiple different delayed-inputs and constraints among generators. Since power systems have various generators under different topologies, it is necessary to reflect the characteristics of multiple-generators in order to improve the dynamic performance of AGC such as stabilizing frequency and maintaining tie-line flows. Specifically, one of major advantages in MPC-based approach is more tractable to realize multi-inputs-multi-outputs (MIMO) system controllers rather than single-input-single-output system based approaches such as PI [19].

Second, most of studies except ref. [24] dealt with a continuous time controller. In the field, control signals in each BA should be periodically updated because EMS is a discretized controller [14]. Moreover, MPC-based approach generally has a computational

complexity due to the optimization process of customized objective functions. Specifically, ref. [23] showed that the average time for optimization in the MPC-based approach increases exponentially as the prediction horizon increases, but the desirable dynamic performance is only obtained when the prediction horizon is large enough. The average time for optimization also increases exponentially as the number of generators increases. Therefore, system operators (or control designers) should consider how to reduce the computational burden caused by MPC-based approach.

CHAPTER 3. MPC-BASED APPROACH FOR AGC

3.1 MPC-BASED APPROACH FOR AGC

This section provides the proposed MPC-based approach for AGC. Considering the spatial structures, both single-area case and multi-area case are developed. Moreover, this section mainly shows the proposed conversion process to convert the delayed-input system models to a delay-free system model and the proposed controller based on a quadratic cost criterion, which is a squared-weighted sum of states (regulated variables: generators' frequencies) and controls (load references set-point) among multiple-generators.

In this part, the subscript *i* (representing each BA) is omitted for brevity. The frequency, load reference, and so on are variables and matrices in each BA. Since the frequency sampling and control processes are activated in a discrete-time manner, we used multiple time scales as shown in Figure. 3.1.

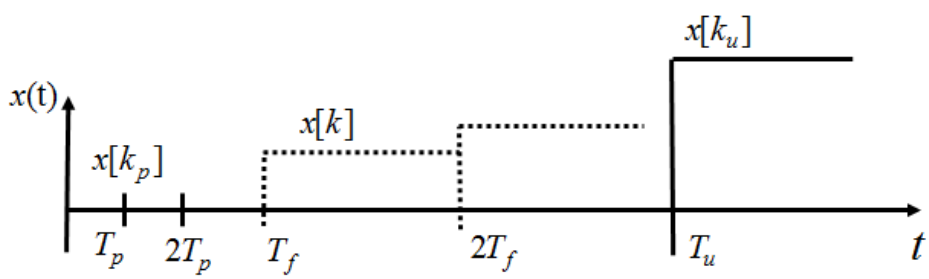

Figure 3. 1 Multiple timescales

3.1.1 SINGLE AREA CONTROL MODEL WITHOUT DELAYED-INPUTS [28]

Without loss of generality, this thesis assumes that random and unknown disturbances d_w in Eq. (2.9) are zero-mean Gaussian noises. From Equation (2.9), the discrete-time frequency model with constraints is described as

$$w_{k+1}=\mathrm{A}w_k + Bu_k \tag{3.1}$$

$$\underline{u} \le u_k \le \overline{u} \tag{3.2}$$

where $w \in \mathbb{R}^n$ is the frequency vector, and $u \in \mathbb{R}^n$ is the control vector. In this case, n is the total number of generators in the power network. Equation (3.2) provides the information of each generator regarding a different and limited load reference ramp rate of each capacity per minute (i.e., combustion turbines can develop ramps of approximately 13% to 28% of their capacity per minute [29]).

From Equation (3.1), the state predictions for N-step horizon are expressed as follows:

$$\begin{aligned}\begin{bmatrix} \hat{w}_{k+1|k} \\ \hat{w}_{k+2|k} \\ \vdots \\ \hat{w}_{k+N|k} \end{bmatrix} &= \begin{bmatrix} A \\ A^2 \\ \vdots \\ A^N \end{bmatrix} w_k + \begin{bmatrix} B & 0 & \cdots 0 \\ AB & B & \cdots 0 \\ \vdots & \vdots & \ddots \vdots \\ A^{N-1}B & A^{N-2}B & \cdots B \end{bmatrix} \begin{bmatrix} u_{k|k} \\ u_{k+1|k} \\ \vdots \\ u_{k+N-1|k} \end{bmatrix} \\ &= M_w w_k + C_u U_k \end{aligned} \tag{3.3}$$

where

$$\bar{w} = [\hat{w}_{k+1|k,}\, \hat{w}_{k+2|k} \cdots \hat{w}_{k+N|k,}]^T$$

$$U_k = [u_{k|k}, u_{k+1|k}, ..., u_{k+N-1|k}]^T$$

M_w is $(N \times n) \times n$ matrix, C_u is $(N \times n) \times (N \times n)$. The attempt to minimize a squared-weighted sum of state (regulated variables) x and controls u of the given Equation (3.3) is described by

$$\begin{aligned} J_k &= \sum_{i=0}^{N-1} \left(\left\| w_{k+i|k} \right\|_Q^2 + \left\| u_{k+i|k} \right\|_R^2 \right) + \left\| w_{k+N|k} \right\|_{Q_N}^2 \\ &= U_k^T H U_k + 2 w_k^T F_w^T U_k + w_k^T G w_k \\ &= U_k^T H U_k + 2 F_{w,1}^T U_k + c_0 \end{aligned} \tag{3.4}$$

where

$$\mathrm{Q}' = \mathrm{diag}\,[Q, Q, \ldots, Q_N]$$

$$\mathrm{R}' = \mathrm{diag}\,[R, R, \ldots R]$$

$$H = C_u^T Q' C_u + \mathrm{R}'$$

$$F_w = C_u^T Q' M_w$$

$$G = M_w^T Q' M_w + Q$$

$$F_{w,1} = w_k F_w$$

$$c_0 = \left(M_x w_k \right)^T \tilde{Q} M_x w_k$$

In Eq. (3.4), Q is weighting matrix for the state, Q_N is weighting matrix for the terminal state, R is weighting matrix for the control, and c_0 can be considered as a constant.

According to the result of Equation (3.4), *N*-horizon optimal control gain K_{mpc} is $-H^{-1}F_{w,1}$ when the system is unconstrained, and the optimal control u_k^* is derived by the first horizon gain.

3.1.2 SINGLE AREA CONTROL MODEL WITH DELAYED-INPUTS

Without loss of generality, this paper assume that random and unknown disturbances d_w in Eq. (2.9) are zero-mean Gaussian noises. Therefore, the discrete-time frequency model with input delays and constraints is described as

$$\begin{aligned}\hat{w}_{k+1|k} &= Aw_k + B_1 u_{1,k-h1} + B_2 u_{2,k-h2} + \ldots + B_n u_{n,k-hn} \\ &= Aw_k + \sum_{l=1}^{n} B_l u_{l,k-h_l}\end{aligned} \tag{3.5}$$

$$\underline{u}_l \le u_{l,k} \le \overline{u}_l \tag{3.6}$$

where $w \in \mathbb{R}^n$ is the state vector for *n*-generators' frequencies, $u \in \mathbb{R}^n$ is the control vector for *n*-generators' load reference ramp rates, B_l is the *l*-th column of *B*, and $h_l > 0$ is a known input delay. Eq. (3.6) provides the load reference ramp constraints of each generator regarding a different and limited ramp rate of each capacity per second.

From Eq. (3.5), the state predictions for *i*-step horizon are expressed as follows:

$$\hat{w}_{k+i|k} = A^i w_k + \sum_{l=1}^{n} \sum_{j=1}^{i} A^{i-j} B_l u_{l,k-h_l+j-1|k} \tag{3.7}$$

When $-h_l + j - 1$ is less than 0, $u_{k-hl+j-1}$ are previous input values and could be considered uncontrollable and known disturbances. Based on MPC-based approach, the state predictions from *k+1* to *k+N* are expressed as below:

$$\begin{bmatrix} \hat{w}_{k+1|k} \\ \vdots \\ \hat{w}_{k+h_v+1|k} \\ \vdots \\ \hat{w}_{k+N|k} \end{bmatrix} = \begin{bmatrix} A \\ \vdots \\ A^{h_v+1} \\ \vdots \\ A^{N} \end{bmatrix} w_k + \begin{bmatrix} \begin{bmatrix} B^1_{old} \end{bmatrix} & \begin{bmatrix} 0 \end{bmatrix} \\ \begin{bmatrix} B^2_{old} \end{bmatrix} & \begin{bmatrix} B_{new} \end{bmatrix} \end{bmatrix} \begin{bmatrix} \begin{bmatrix} U^{pre} \end{bmatrix} \\ \begin{bmatrix} U_k \end{bmatrix} \end{bmatrix} \tag{3.8}$$

where

$$U^{pre} = [u_{k-hp}, u_{k-hp+1}, \dots\ u_{k-1}]^T$$

where h_v is the minimum delayed input time among generators, h_p is the maximum delayed input time among generators.

Based on Eq. (3.8), the predictive states, which are affected by the future control set U_k, could be re-expressed as follows:

$$\bar{w} = M_w w_k + C_u U_k + D_s U^{pre} \tag{3.9}$$

where

$$\bar{w} = [\hat{w}_{k+hv+1|k,}\ \hat{w}_{k+hv+2|k} \cdots \hat{w}_{k+N|k,}]^T$$

$$U_k = [u_{k|k}, u_{k+1|k}, \dots, u_{k+N-hp-1|k}]^T$$

$$M_w = [A^{hv+1},\ A^{hv+2}, \dots,\ A^N]^T$$

$$C_u = B_{new}$$

$$D_s = B^2_{old}$$

Based on this process from Eq. (3.8) to Eq. (3.9), the delayed-input system can be handled as a delay-free system with a certain (known) disturbance $D_s\ U^{pre}$.

Given Eq. (20), the objective of the finite state prediction horizon N is developed to minimize quadratic cost criterion J_k, a squared-weighted sum of states $\bar{w}_G$ and controls U_k. This attempt of Eq. (3.9) is described by

$$\begin{aligned} J_k &= \sum_{k=1}^{N-h_v-1} \left\| \hat{w}_{k+h_v|k} \right\|_Q^2 + \left\| w_{k+N|k} \right\|_{Q_N}^2 + \sum_{k\in\Omega} \left\| u_{k|k} \right\|_R^2 + \sum_{k\in\Omega^c} \left\| u_{k|k} \right\|_{R_M}^2 \\ &= U_k^T \tilde{R} U_k + \bar{w}^T \tilde{Q} \bar{w} \\ &= U_k^T H U_k + 2(F_w^T + F_s^T) U_k + c_1 \\ &= U_k^T H U_k + 2F_{w,1}^T U_k + c_1 \end{aligned} \tag{3.10}$$

where

$$\Omega = \left\{0,\ T_u/T_f,\ 2\cdot T_u/T_f, \ldots\right\}$$

$$\Omega \cup \Omega^c = \left\{k \mid 0 \le k \le N - h_p,\ k \in \mathbb{Z}\right\}$$

$$\tilde{\mathrm{Q}} = \mathrm{diag}\,[Q, Q, \ldots, Q_N]$$

$$\tilde{R} = \mathrm{diag}\,[R, R_M, R_M, \ldots, R, R_M, R_M, \ldots]$$

$$H = C_u^T \tilde{Q} C_u + \tilde{R}$$

$$F_w = C_u^T \tilde{Q} M_w w_k$$

$$F_s = C_u^T \tilde{Q} D_s U^{pre}$$

$$c_1 = \left(M_x w_k\right)^T \tilde{Q} M_x w_k + \left\{2\left(M_x w_k\right)^T + \left(D_s U^{pre}\right)^T\right\} \tilde{Q} D_s U^{pre}$$

R_M are weighting matrices where R_M has a larger weighting than R. Through R_M, the control gain is almost 0 when k is in Ω^c. That is, the multiple-horizon control signal set U_k has nonzero values only when $k \in \Omega$.

Based on Eq. (3.10), the multiple-horizon control signal set U_k is computed. Since the control signal u_k is the load reference set-point ramp rate per T_f, rather than T_u, the transmitted control signal u_{k_u} for generators is calculated as follows:

$$u_{k_u} = u_k \frac{T_f}{T_u} \tag{3.11}$$

3.1.3 MULTI-AREA CONTROL MODEL WITH CONSIDERING TIE-LINE FLOWS

3.1.3.1 TIE-LINE FLOW MODEL

An electric power system network is formed by BAs interconnected through the transmission lines between areas. The area-wide dynamics is coupled through tie-line power flows based on Eq. (2.1), and the tie-line power flows should be controlled.
The power flow on a single tie line from *i* bus to *j* bus is given in [14]:

$$P_{ij} = \frac{E_i E_j}{X_{ij}} \sin(\delta_i - \delta_j) \tag{3.12}$$

Linearizing an initial operating point represented by $\delta_i = \delta_{i0}$ and $\delta_j = \delta_{j0}$, we obtain $\Delta P_{ij} = J_{ij}\Delta\delta_{ij}$, where $\Delta\delta_{ij} = \delta_i - \delta_j$ and $J_{ij} = (E_i E_j / X_{ij})\cos(\delta_{i0} - \delta_{j0})$. Basing on this approach, the several tie-line power flows P_f could be described as

$$P_f = \begin{bmatrix} J_{fG} & J_{fL} \end{bmatrix} \begin{bmatrix} \delta_G \\ \delta_L \end{bmatrix} \tag{3.13}$$

The phase angles on load buses can be expressed in terms of the phase angles on generator buses and the demands on load buses:

$$\delta_L = -J_{LL}^{-1}(J_{LG}\delta_G + P_L) \tag{3.14}$$

Substituting Equation (3.14) into Equation (3.13) eliminates the load bus phase angles. Based on this result, Equation (3.15) can be obtained as follows:

$$\begin{aligned} P_f &= (J_{fG} - J_{fL} J_{LL}^{-1} J_{LG})\delta_G - J_{fL} J_{LL}^{-1} P_L \\ &= K_f \delta_G + D_f P_L \end{aligned} \tag{3.15}$$

3.1.3.2 MPC-BASED APPROACH FOR AGC CONSIDERING TIE-LINE FLOWS

Based on Eq. (3.4) and (3.10), it is impossible to maintain tie-line flows to a scheduled value. Therefore, we consider the additional process to control tie-line flows.

Based on Eq. (3.15), EMS only has the controllability of angles δ by adjusting the power outputs of generators in its area. However, the angles are affected by the power deviations in other areas. Therefore, EMS cannot maintain individual tie-line power flows to scheduled values without considering the centralized scheme[1]. In the field, given that developing the centralized structure among bulk BAs is impractical, each BA controls the net of tie-line power flows from its area to neighboring BAs. On the basis of this tie-line control scheme, the tie-line control action in each BA is not a topological problem and is another form of active power balancing in each BA [28].

Basing on Eq. (2.14), this paper proposes the pseudo-frequency at *i*-BA, which is described by

$$w_{i,G}^{ps}[k_u] = w_{i,G}[k_u] + H_i P_{i,f}^{net}[k_u] \tag{3.16}$$

where H_i is a diagonal matrices with $1/\beta_i$. This scheme is based on the same principle as ACE in traditional PI-based AGC. This pseudo-frequency substitutes the measured frequency $w_{i,G}$ in Eq. (3.1) or Eq. (3.5) while EMS computes AGC signals [28].

[1] Appendix A

3.1.4 CONTROL STRUCTURE

Figure 3.2 shows the control loop of the proposed MPC-based approach for AGC when there are multiple-generators. It uses multiple inputs, which are generators' frequencies and tie-line flows, and multiple outputs are computed by considering the future state errors which are the predictive frequency errors $\overline{w}$.

As mentioned before in Section 2.3, a major difference between the MPC-based and PI-based approaches is that control designers may select the essential information from the available data in the system based on the objective and constraints, and design the controller to satisfy the system requirements. Therefore, the model block is very important to improve the dynamic performance and satisfy the system requirements.

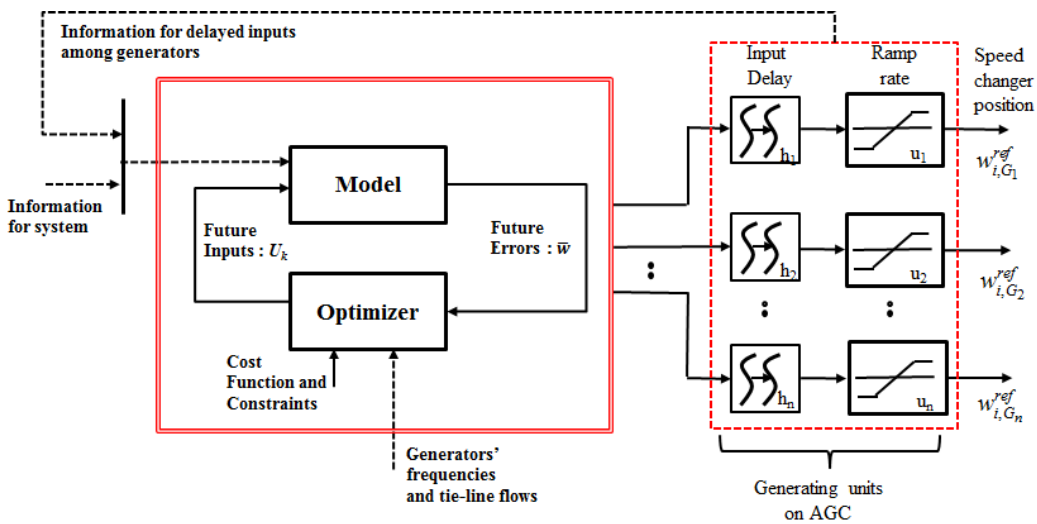

Figure 3. 2 Proposed MPC-based approach for AGC

3.2 COMPUTATIONAL COMPLEXITY IN MPC

This section provides the bulk-area portioning scheme in order to reduce the computational burden, which is one of major drawbacks in MPC-based approach.

3.2.1 COMPUTATIONAL COMPLEXITY

Computing problems come in different varieties; some are easy, and some are hard. For example, the sorting problem is an easy one. Say that we need to arrange a list of numbers in ascending order. Even a small computer can sort a million numbers rather quickly. Compare that to a scheduling problem. Say that we must find a resource allocation schedule to satisfy some reasonable constraints, such as that the allocated resources should be equal to the demands at each time [30]. Specifically, computational complexity grows exponentially in the number of optimization variables [31].

In MPC-based approach, the computational complexity can be a great problem since it deals with the control schedule to minimize future errors as shown in Figure 2.5. Since the number of optimization variables in MPC-based approach depends on the prediction horizon sizes and the system size, a centralized control scheme for a bulk-system is impractical and undesirable [23, 24].

There are two ways in order to reduce the computational complexity [31].

One way of speeding up the solution of the optimization problem is to use QP solvers tailored for MPC, where the special structure of the Karush–Kuhn–Tucker system is used to decrease the complexity of the algorithm. Basically two approaches can be used. First, general methods utilizing the structure in block-banded equation systems can be used. Second, Riccati recursions can be used. Based on these approach, the algorithms for solving

QP becomes much tractable, and the complexity of the algorithms is reduced in comparison to the other optimization algorithms such as dynamic programming and evolutionary algorithms. However, this way has still a significant weak-point when the number of optimization variables are large.

Another way of reducing the on-line computational effort is to precompute the control law. Briefly, the procedure can be described as that the state-space is partitioned into a number of regions, where in each a different affine control law is optimal [32]. This approach can effectively reduce the number of optimization variables in comparison to the original problem. However, it is necessary to coordinate resource allocation among the distributed (participated) regions.

In this thesis, QP algorithm is adopted in order to reduce computing time of the cost minimization as shown in Eqs. (3.4) and (3.10). However, it has still a significant weak-point since a number of generators are usually participated in AGC. Therefore, this thesis proposes the scheme to divide the original state-space based on coordinating resource allocation among the distributed (partitioned) regions.

3.2.2 BULK AREA PARTITIONING SCHEME

Figure 3.3 shows the type of spatial separation which this thesis proposes. In the proposed scheme, each subsystem (partitioned system) in a bulk BA has its own AGC scheme in EMS, such as a BA, and the net tie-line flows among subsystems is recomputed by the upper controller in its BA [28]. The net of tie-line flows among subsystems is described as

$$\Delta P_{i_s,k}^{net} = \sum_{j=1}^{n_A} \Delta P_{ij}[k] + \left(\Delta P_{m,i_s}^{net}[k_m] - \sum_{k=1}^{n_i} \frac{\alpha_k}{n_i} \Delta P_{m,i_k}^{net}[k_m] \right) \tag{3.17}$$

$$\sum_{k=1}^{n_i} \alpha_k = n_i \tag{3.18}$$

$$0 \le \alpha_i \le n_i \tag{3.19}$$

where n_A is the number of BAs, n_i is the number of subsystems in BA i, α_k/n_i is the participation rate for balancing in subsystem k in BA i, $P_{i_s j}$ is the power flow from subsystem i_s to BA (or subsystem) j, k_m is the discretized mechanical power sampling time step, and $\Delta P_{m,i_k}^{net}$ is the net of deviated mechanical power output in subsystem i_k. According to this control scheme, each subsystem equally reacts to the discrepancy between the generation supply and the total MW obligation in its BA when $\alpha_i = 1$ for every i.

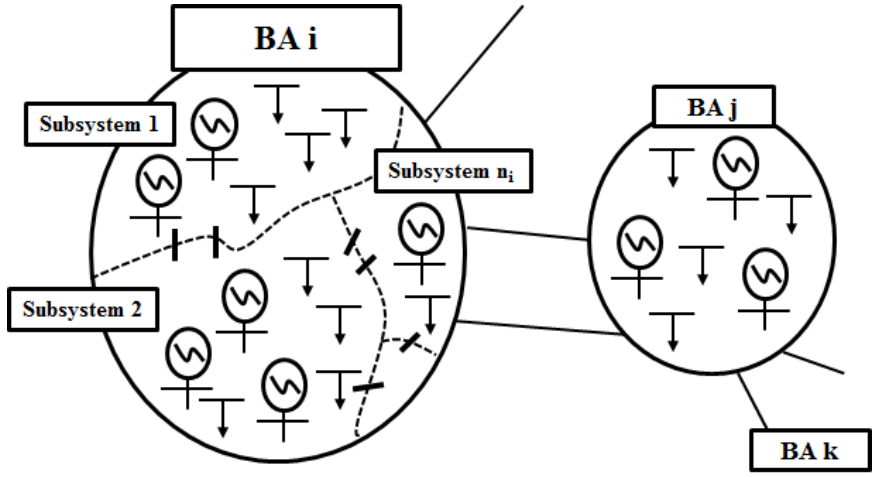

Figure 3. 3 Bulk area partitioning at BA *i*

3.3 DISCRETIZED CONTROL MODELS FOR A CONTINUOUS SYSTEM

In this section, we describe a continuous dynamics model controlled by discretized and distributed signals computed by both PI-based approach and MPC-based approach.

3.3.1 PI-BASED APPROACH

In the field, most real-world AGC systems use PI-based controllers, and control output signals are developed to minimize area control errors (ACEs), which represent the discrepancy between generation supply and total megawatt (MW) obligation in each BA [1]. The discretized ACE can be described as

$$ACE[k_p] = \beta_i w_{i,G}^{rep}[k_p] + P_{i,f}^{net}[k_p] \tag{3.20}$$

where $w_{i,G}^{rep}$ is the representative frequency at area i, and β_i is the frequency bias factor, and $P_{i,f}^{net}$ is the net tie-line flow at area i. In PI-based approach, ACE is integrated for every sampling time and multiplied the control gain K_i. Unconstrained load reference set-point can be described as

$$w_G^{ref}[k_u + 1] = K_i \left\{ Z^{-1} \left\{ \left(\frac{1}{1 - z^{-1}} \right) F(z) \right\} \right\} \tag{3.21}$$

where $F(z)$ is a Z-transform of the signal $f[k_p]$ which is defined as $T_p \cdot ACE[k_p]$, T_p is a frequency sampling time, Z^{-1} is the inverse Z-transform and K_i is an integral gain. Since

there are the load reference ramp rate limits among generators, the controller should consider Eq. (15) such as

$$\underline{u} \le \frac{w_G^{ref}[k_u+1] - w_G^{ref}[k_u]}{T_u} \le \overline{u} \tag{3.21}$$

Figure 3.4 shows the PI-based controller in distributed systems where Φ is the function to accumulate ACE via Eq. (3.21). In practice, the load reference w_G^{ref} is periodically updated at each sampling time T_u, and the frequency is sampled at each T_p.

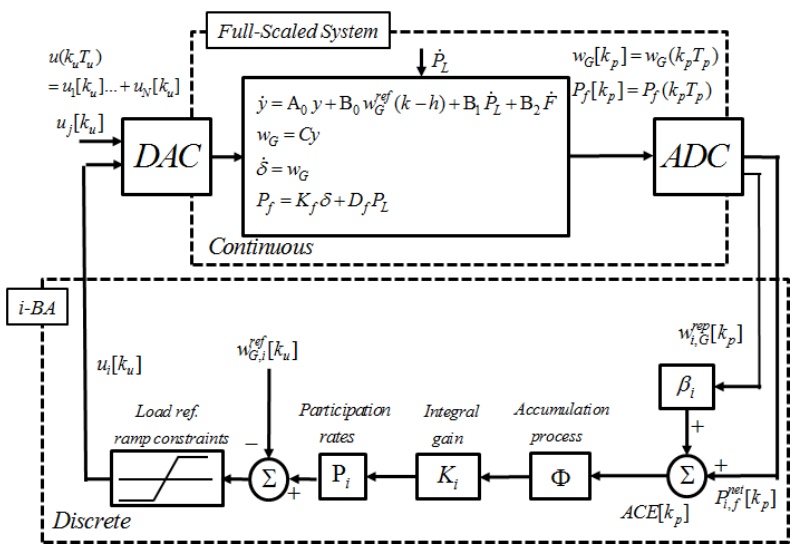

Figure 3. 4 The Conventional PI-based approach for AGC

In this controller, the EMS in BA i controls the power outputs of participating generators based on the area system frequency $w_{i,G}$, with no information on the frequencies of other areas. The full dynamic network system is impacted by the control inputs provided by each BA.

3.3.2 THE PROPOSED MPC-BASED APPROACH

Figure 3.5 shows the proposed MPC-based approach for AGC in distributed systems, where S_i is the function to select the control at the first horizon and compute $u[k_u]$ via Eq. (3.11), U^{pre} is the previous control input set in Eq. (3.9), and T_i is the function to compute $H_i P_{i,f}^{net}$ from the individual tie-line flows in i-BA.

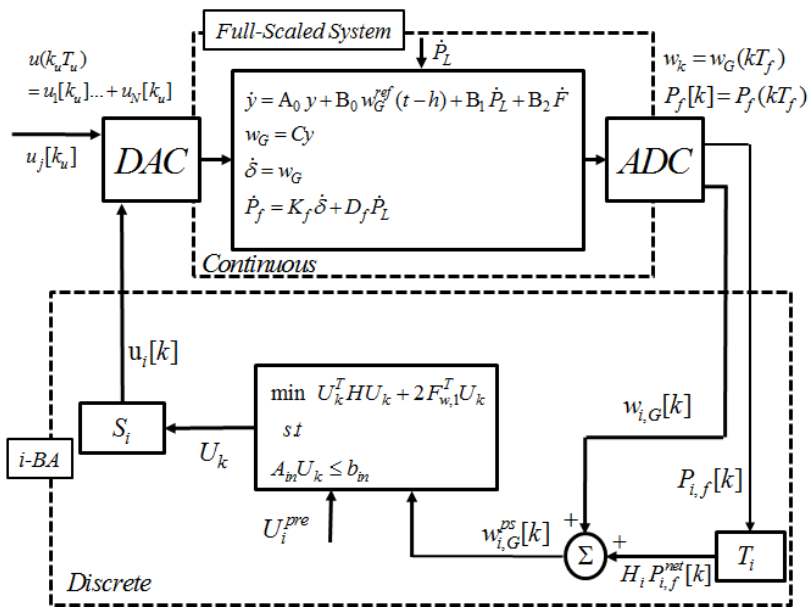

Figure 3. 5 The Proposed MPC-based approach for AGC

The terms A_{in} and b_{in} express the load reference ramp constraints of generators. When i-BA is partitioned into a number of regions, the function T_i in Figure 3.5 includes the control process for Equation (3.17).

CHAPTER 4. ILLUSTRATIVE EXAMPLES

4.1 RESULTS IN A UNIT-STEP DISTURBANCE

4.1.1 SIMULATION SETTING AND PRIMARY CONTROL RESULTS WITHOUT AGC

Here we describe a simulation involving three conventional generators in a five-bus system, as shown in Figure 4.1. Table 4.1 lists the generator parameters and initial operating points for each bus: i.e., the voltages, angles, and power. Table 4.2 lists the scheduled tie-line flows at the initial time. All transmission lines had an impedance of 0.01 + j0.1 pu, except for tie-lines (3) and (6), which had an impedance of 0.1 + j1.

These simulations were carried out to investigate both the conventional PI-based AGC and the proposed MPC-based AGC when a step increase in the load of 0.2 pu occurs at Bus 4 at time t = 1 s. According to the previous researches [4-9], it is shown how the integral gain affects the control performance via two different values, and the proposed MPC-based simulation results are analyzed by comparison with the PI-based control results from the perspective of dynamic control performance: i.e., the frequency settling time, the quantity of inadvertent tie-line flows. Both control approaches are simulated with four scenarios based on load reference ramp constraints and input time delays: (a) without load reference ramp constraints and without delayed inputs, (b) with load reference ramp constraints and without delayed inputs, (c) without load reference ramp constraints and with delayed inputs, and (d) with load reference ramp constraints and with delayed inputs.

The simulated frequency deviations differed among generators in the power system. The frequencies of all generators fell at time t = 1 s. The decreases in frequency of Gens 1 and 2 were larger than those of Gen 3 because Gens 1 and 2 were located with shorter electrical distances from the disturbance at Bus 4. Governors on generators act only to maintain

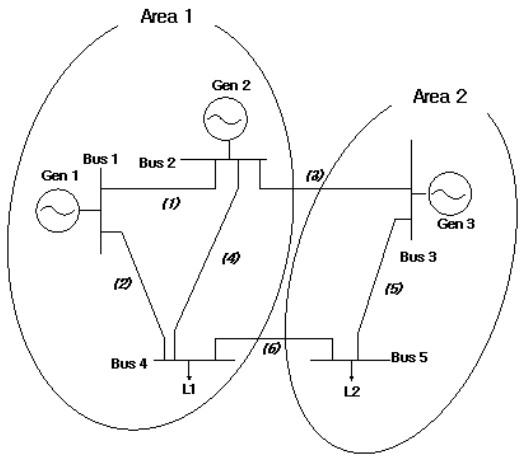

Figure 4. 1 Five-bus system (Two areas)

Table 4. 1 Parameters for the five-bus simulation in per unit

Bus	#1	#2	#3	#4	#5
V	1	1	1	0.975	0.970
δ	0	0.008	−0.042	−0.048	−0.107
P	0.41	0.70	0.60	−1	−0.7
M	2	3	2	-	-
D	5	5	5	-	-
T_g	0.25	0.25	0.25	-	-
T_a	0.2	0.2	0.2	-	-
K_t	250	250	250	-	-
r	20	15	20	-	-
h	7	3	4	-	-

Table 4. 2 Initial tie-line power flows

	From Bus	To Bus	Active Power [pu]
Area 1 to Area 2	2	3	0.050
	4	5	0.055

frequency, and the frequencies of all generators eventually converged to a common value of -3.71 mpu, even though the initial behavior differed among generators. Therefore, AGC is necessary to stabilize the deviated frequency, -3.71 mpu. Specifically, this is the primary objective of AGC [14].

4.1.2 TRADITIONAL PI-BASED APPROACH

Table 4.3 lists the data and parameters for PI-based control simulation. We assume that each generator has the same load reference ramp constraint, i.e., $|u| \leq 3 \times 10^{-4}$ pu/s. Examples of the impacts, set by two different integral gains, are shown in Figures 4.2 and 4.3. These results shows how the integral gain affects the control performance over each scenario.

Table 4. 3 Parameters for PI-based AGC for each BA

		BA 1	BA 2
Discretized control update time [s]	T_p	10^{-3}	10^{-3}
	T_u	2	2
Frequency Bias Factor	β_i	50	25
Representative frequency	$w_{i,G}^{rep}$	Gen2	Gen3
Participation rate of generator j	ρ_j	0.5	1
Integral Gain	Case I : K_i	-0.008	-0.012
	Case II : K_i	-0.002	-0.003
Load Ref. Ramp Constraints [pu/s]	u^{max}	3×10^{-4}	3×10^{-4}
	u^{min}	-3×10^{-4}	-3×10^{-4}

With the conventional PI-based approach, tuning of the integral gain is very important to secure good dynamic performance and to maintain the frequency and the tie-line flows. Specifically, Fig. 4.2 shows that each scenario (i.e. system conditions) had significantly different results via a large integral gain. The deviations of the frequencies and tie-line flows shown in Fig. 4.2(a) were shorter-lived than those shown in Fig. 4.3(a), which shows that the AGC signals with a large integral gain exhibited better dynamic performance than with a small integral gain. However, the time-delayed system shows better performance with a smaller integral gain, as can be seen by comparing Figs. 4.2(c) and 4. 3(c). Moreover,

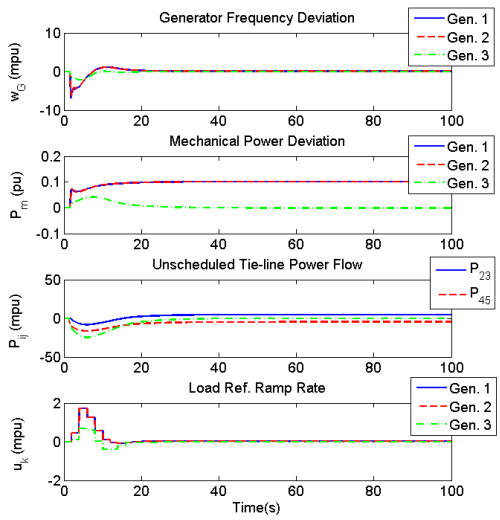

(a)

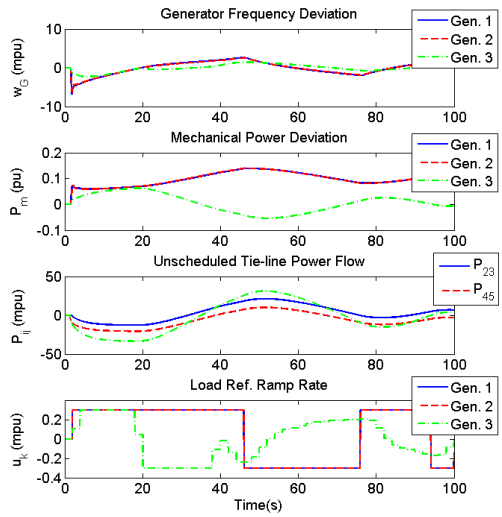

(b)

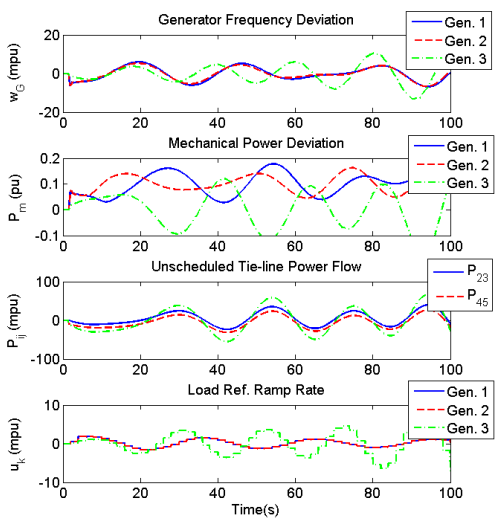

(c)

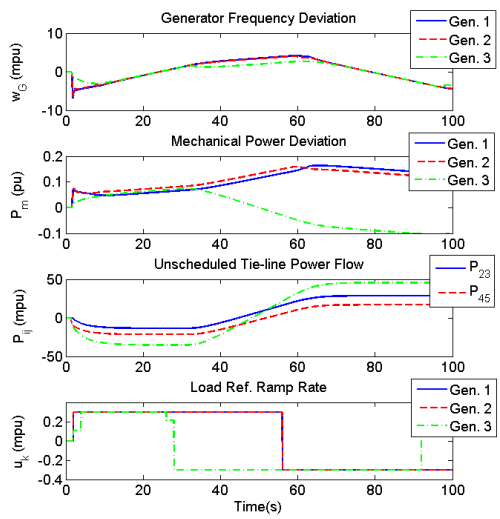

(d)

Figure 4. 2 PI-based simulated AGC data in four scenarios with Case I: A Large Integral Gain

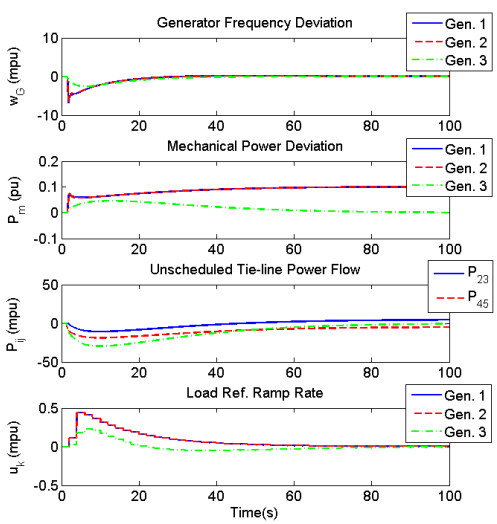

(a)

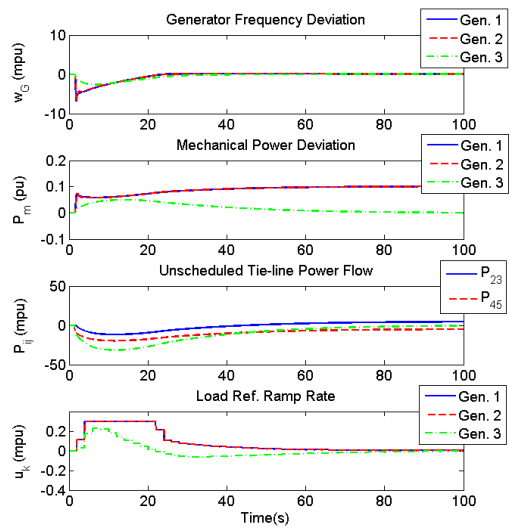

(b)

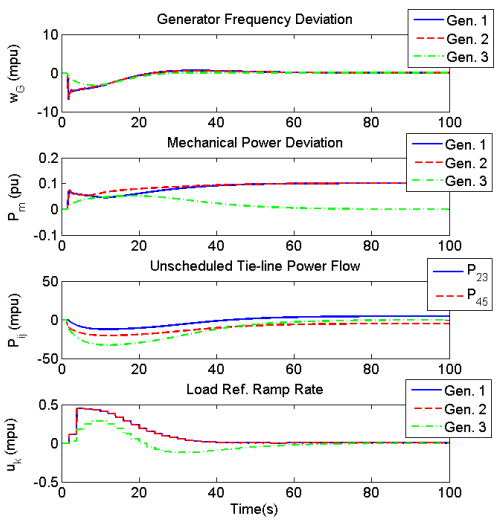

(c)

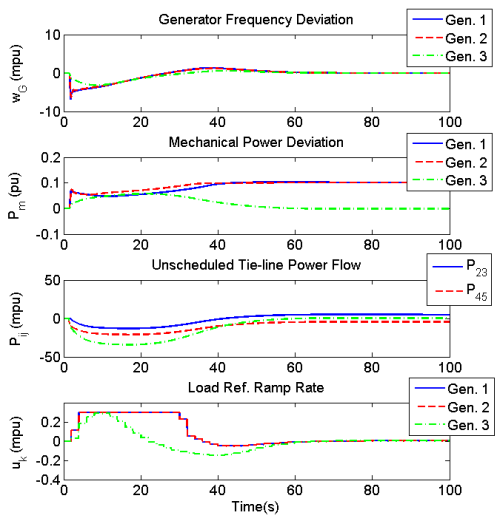

(d)

Figure 4. 3 PI-based simulated AGC data in four scenarios with Case II: a Small Integral Gain.

the results in Fig. 5(c) were unstable. This signifies that the PI-based approach for AGC has an operational risk from setting a large integral gain to improve the dynamic performance as mentioned in previous researches. Specifically, it shows poor control when generators had the load reference ramp constraints and delayed inputs. As an interesting aspect in Fig. 4.3, the PI-based approach with a small integral gain is not largely affected by the changes of system conditions even though it provides poor control results.

The PI-based approach for highly interactive MIMO systems is very difficult. Specifically, PI-based approach for AGC in each BA commonly requires the single information, ACE. Even though it has information such as characteristics of multiple-generators and network model, it does not provide effective method to use the information in real-time since it is a single-input-single-output (SISO)-based scheme. Specifically, as shown in Figures. 4.2 and 4.3, Gens 1 and 2 participated equally in AGC. With no loss of generality, the participation rates ρ_j should be changed based on the speed of response and the constraints of the generators; however, they are usually fixed constant values in the field.

There are two different approaches to improve the dynamic performance of PI-based controller. If it is required to improve dynamic performance for AGC in PI-type designs, both integral gain for PI and participation factors of each participating generators in AGC should be tuned in real-time. Specifically, tuning integral gain is closely related to consider input delays among generators, and tuning participating factors is closely related to consider generators' load reference ramp rates. As mentioned in this thesis, traditional tuning algorithms for PI-based approaches for AGC were widely apodted with artificial intelligence algorithms such as fuzzy and neural network algorithms [33-36]. However, artificial intelligence algorithms are usually time-consuming works and may become trapped in local optimal solutions or require long solution times. As a result, PI-based AGC suffers from real-time dynamic resource allocation problems.

4.1.3 PROPOSED MPC-BASED APPROACH

Table 4.4 lists the data and parameters used in the MPC-based control simulation (i.e., the method described here). In the derivation of Eq. (20), we assumed that $N > h_p/T_f$; i.e., the minimum prediction horizon should be larger than the previous input horizon. In the optimization process for minimizing Eq. (21), we set $|u| \leq 6 \times 10^{-4}$ pu/s because $T_u = 2$ s and $T_f = 1$.

Table 4. 4 Parameters for MPC-based AGC for each BA.

	Parameters	BA 1	BA 2
Discretized control update time [s]	T_f	1	1
	T_u	2	2
Load Ref. ramp Constraints [pu /s]	$\overline{u}$	3×10^{-4}	3×10^{-4}
	$\underline{u}$	-3×10^{-4}	-3×10^{-4}
Weighting Matrix	Q	$10^2 I$	10^2
	Q_N	$10^2 I$	10^2
	R	I	1
	R_M	$10^4 I$	10^4
	Q_f	$10^2 I$	10^2
Prediction Horizon	N	20	20

- I is a 2-by-2 identity matrix

Figure 4.4 shows the generators' frequency behaviors of the proposed MPC-based approach in each scenario. The results shows that it has the advantage that good dynamic performance can be achieved. As listed in Table 4.5 and Table 4.6, the settling times and the quantity of the deviated frequency with the MPC-based approach were shorter and smaller than with the PI-based approach. These data show that the dynamic performance of AGC can be improved using the MPC-based approach. Moreover, because of the conversion process from Eq. (19) to Eq. (20), the control system was not severely impacted

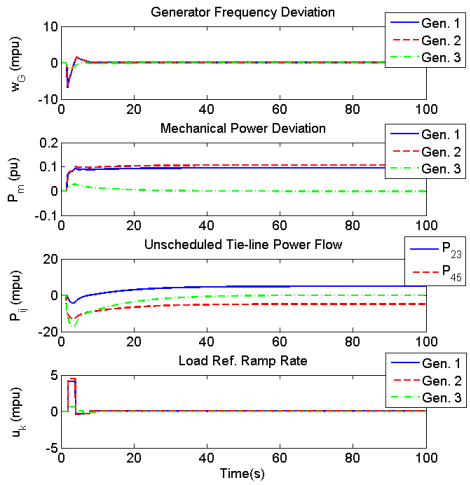

(a)

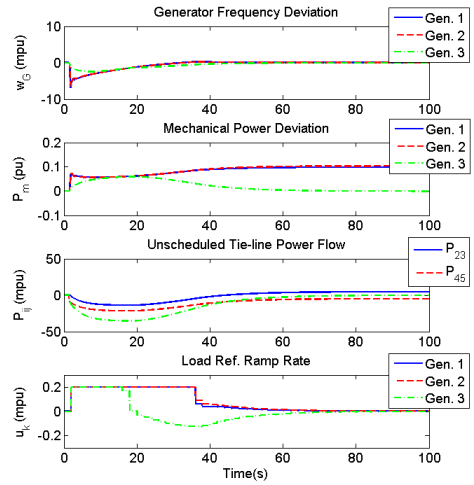

(b)

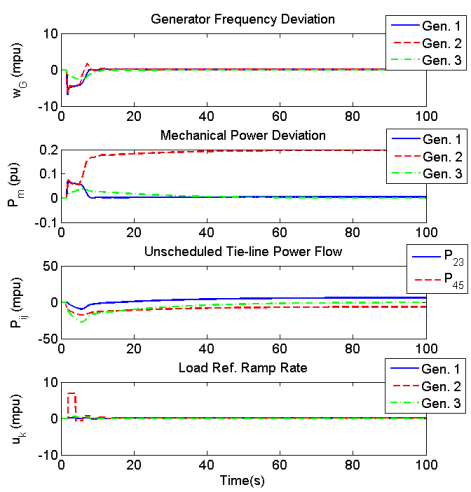

(c)

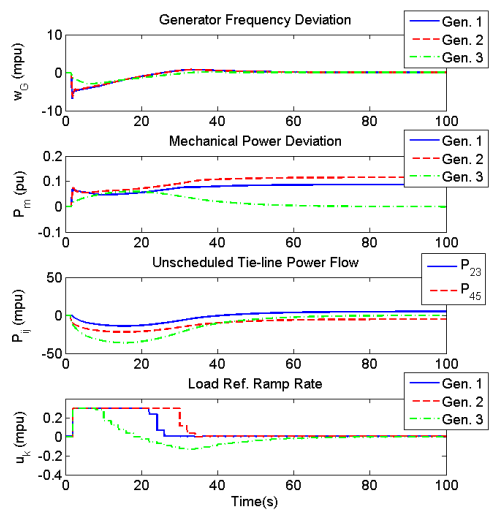

(d)

Figure 4. 4 MPC-based simulated AGC data in four scenarios

by handling constraints as well as delayed inputs among generators, in contrast with the conventional PI-based approach.

This control scheme depends on the dynamics of the frequency responses of the generators. As shown in Figure 4.4, Gen 2 was more active in AGC than Gen 1 due to the lack of restrictions in terms of load reference control. In this case, Gen 2 exhibited one large load reference ramp rate signal (i.e., 7.2 mpu/s during 2–4 s), which was significantly larger than the constrained load reference value 0.3 mpu/s. Note that Gen 1 was not active in AGC during the same time period because not only did Gen 1 have a larger generation output delay (h = 7 s compared with h = 3 s for Gen 2), but the control signal u had no limitation. This shows that the quadratic cost in Eq. (21) can be mainly minimized using Gen 2. However, as shown in Figure 4.4(d), Gen 1 was active in AGC. In this case, Gen 2 was limited in minimizing the quadratic cost function in Eq. (21) due to the load reference ramp rate constraints of Gen 2. Therefore, the MPC-based controller activated Gen 1 to minimize the cost function in Eq. (21), even though Gen 1 had a large generation output delay of 7 s. These data show that the proposed control scheme automatically determined the participation rates based on the speed of the generation output response and the constraints among generators.

Minimizing inadvertent tie-line flows is a necessary part of power system management. Table 4.6 lists the absolute quantities (i.e., total energy) associated with inadvertent tie-line flows during the first 200 s of the simulation. These results show that tie-line flows were maintained using the MPC-based approach. Under normal circumstances, system operators in each BA will pay back the accumulated inadvertent interchanged energy megawatt-hour for megawatt-hour. However, the value of electrical energy varies with time and depends on the scenario. As a result, the profits (or benefits) from the interconnection are strongly influenced by the dynamic performance. Therefore, the MPC-based AGC system described

Table 4. 5 Frequency settling time. (*s*).

		(a)	(b)	(c)	(d)
T_{st}	PI-based (Case I)	12.662	95.362	N/A	N/A
	PI-based (Case II)	19.802	20.679	19.947	44.003
	MPC-based	6.466	19.695	11.345	23.291

* T_{st} : The time required for every generator frequency curve to reach and stay within a range of certain percentage 0. 1% (1 mpu) of the nominal frequency.
* N/A :Non-available

Table 4. 6 Quantity of deviated frequency at Gen 2 until 200 *s*.

		(a)	(b)	(c)	(d)
I_f [pu·s]	PI-based (Case I)	0.0226	0.1325	1.3348	0.6570
	PI-based (Case II)	0.0516	0.0535	0.0701	0.0840
	MPC-based	0.0170	0.0495	0.0336	0.0738

* $I_f\ [k_p+1] = I_f\ [k_p] + T_p\left|w_{2,G}[k_p]\right|$, where T_p= 1 *ms*; $I_f\ [k_p] = 0$ when k_p=0.

Table 4. 7 Quantity of inadvertent tie-line flows until 200 *s*.

		(a)	(b)	(c)	(d)
Q_{tie}^{abs} [pu·s]	PI-based (Case I)	0.324	1.771	21.686	5.098
	PI-based (Case II)	1.130	1.130	1.131	1.141
	MPC-based	0.1322	0.8372	0.3448	1.173

* $Q_{tie}^{abs}[k_p+1] = Q_{tie}^{abs}[k_p] + T_p\left|P_{1,f}^{net}[k_p]\right|$, where T_p= 1 *ms*; $Q_{tie}^{abs}[k_p] = 0$ when k_p=0.

here can help the system operator to maintain the tie-line flows and increase profits by exploiting the interconnections.

The proposed MPC-based control scheme effectively reduced the control quantity via Eqs. (3.4) and (3.10). Figure 4.5 shows that accumulated control signals at each scenario

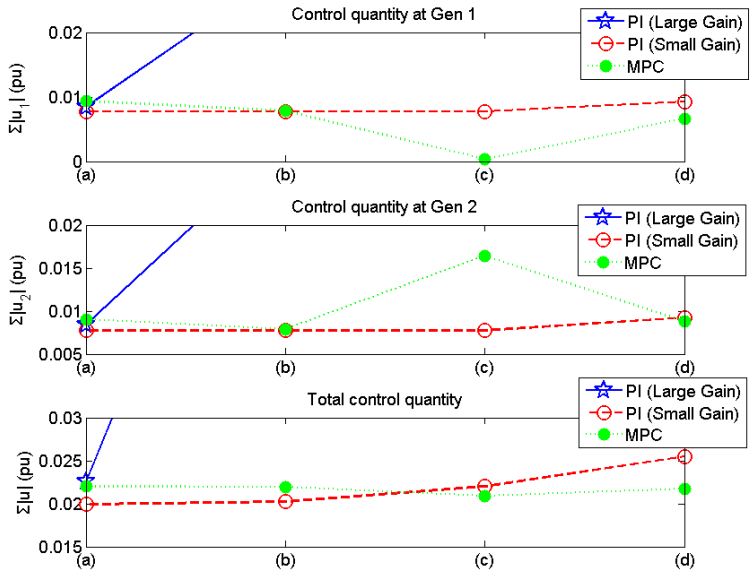

Figure 4. 5 Quantity of control signal

are changed. Even though PI-based approach with a small integral gain had the competitiveness of reducing total control quantity at scenarios (a) and (b), its performances were much lower than MPC-based approach as shown in Tables 4.5 and 4.6. Therefore, it is difficult to directly compare the superiority among the control models, but the proposed MPC-based approach has an advantage to reflect the relationship between the objective variables (frequency states) and the control inputs. If control costs were very high, then the weighting matrix R in Eqs. (3.4) and (3.10) should be set by a high value. As an interesting result, the total control quantity in MPC-based approach did not largely depend on the system condition in comparison to the conventional PI-based approaches since the proposed MPC-based approach can consider the previous inputs to prevent the excessive control inputs.

The MPC-based control scheme described here provides optimal solutions by solving a constrained QP problem. This algorithm provides necessary and sufficient conditions for optimality because it is a convex optimization problem with differentiable objective and

constraint functions, which satisfy Slater's condition [37]. As discussed above, the conventional PI-based approach to AGC does not provide optimality because determining parameters including the integral gain depends on experience and is a trial-and-error process.

4.2 RESULTS IN CONTINUOUS DISTURBANCES

4.2.1 SIMULATION SETTING AND CONTINUOUS LOAD MODEL

4.2.1.1 SIMULATION SETTING

In this simulation, we investigate the effects of the frequency control systems over a period of approximately 4 hours. Both control approaches are simulated with four scenarios based on load reference ramp constraints and input time delays: (a) without load reference ramp constraints and without delayed inputs, (b) with load reference ramp constraints and without delayed inputs, (c) without load reference ramp constraints and with delayed inputs, and (d) with load reference ramp constraints and with delayed inputs.

4.2.1.2 Continuous Load Model

We assumed that power demands at Bus 4 and 5 follow stochastic Ornstein-Uhlenbeck process, i.e.,

$$dP_{L,t}^{i} = \theta(\mu - P_{L,t}^{i})dt + \sigma_i dW_t \tag{4.1}$$

where θ, μ and σ_i are parameters and W_t denotes the Wiener process. In this case, we assume that power demands at each bus do not have the tendency, but its long-run mean is 0 since it can be offset by economic dispatch as another control process in system operation.

Accordingly, Table 4.7 lists the parameters for the stochastic processes in each load bus, and Figure 4.6 shows the demands for a 5-minute period for each bus.

Table 4. 8 Parameters for the stochastic processes at each bus

		Bus4	Bus5
Discretized sample time [s]	dt	0.5	
Mean Reverting Ratio	θ	0	
Long Run Mean	μ	0	
Process Volatility	σ_i	1.5×10^{-2}	0.9×10^{-2}

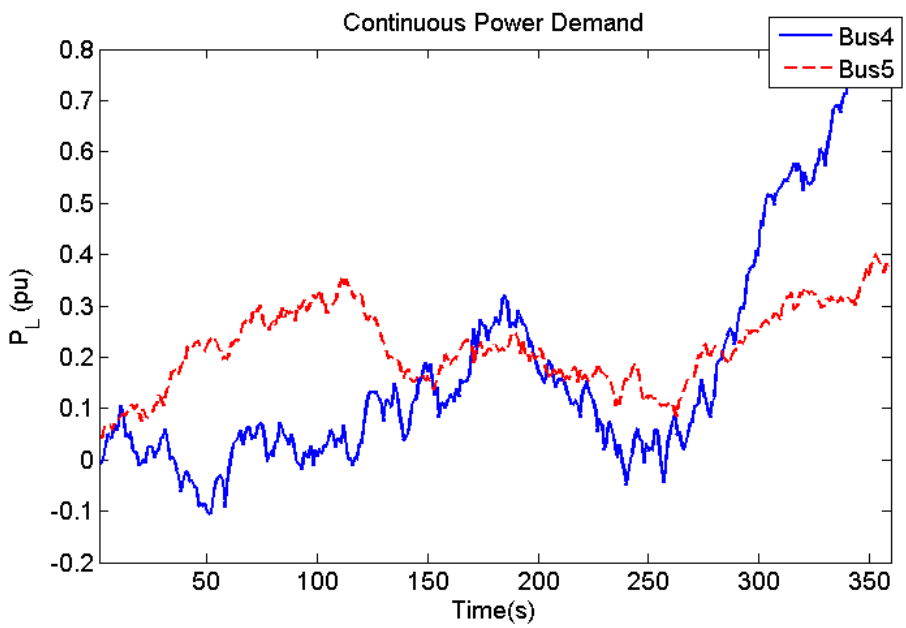

Figure 4. 6 Continuous power demands at each bus

4.2.2 SIMULATION RESULTS

4.2.2.1 FREQUENCY AND ACE RESULTS

Figures 4.7, 4.8, 4.9 and 4.10 show the results of the frequency control systems for each scenarios over a period of approximately 4 hours. In simulation, the sampling time of frequency and ACE was 2 s.

The MPC-based AGC method has the advantage that good dynamic performance of stabilizing frequency. Figures 4.7 and 4.8 show the frequency results for BA1 with load reference constraints and input time delays. Specifically, a large integral gain with the PI-based approach in Figure 4.7 provided conflicting results with delayed inputs. In the field, the degree of frequency deviations is very important in power system since mechanical devices such as steam turbine can be damanged and change the power angles among generators [1]. Therefore, the results in MPC-based approach are very helpful for the system operators who are in charge of stabilize the frequency.

In the simulation results, the settling times in Table 4.5 were closely related to the degree of frequency deviations in Figure 4.7. With no loss of generality, the control inputs should accurately reflect the required power demand based on frequency and tie-line flows. In the previous simulation, the reason the settling times in MPC-based approach were better than conventional PI-based approach is because of considering the future frequency errors based on the proposed predictive model. Therefore, MPC-based approach was able to provide more accurate control input signals compared with the PI-based AGC. For such a reason, the MPC-based approach in a continuous load model provided better results.

ACE results has showed similar results by comparison with the frequency results because ACE is computed by the deviated frequency and the inadvertent tie-line flows.

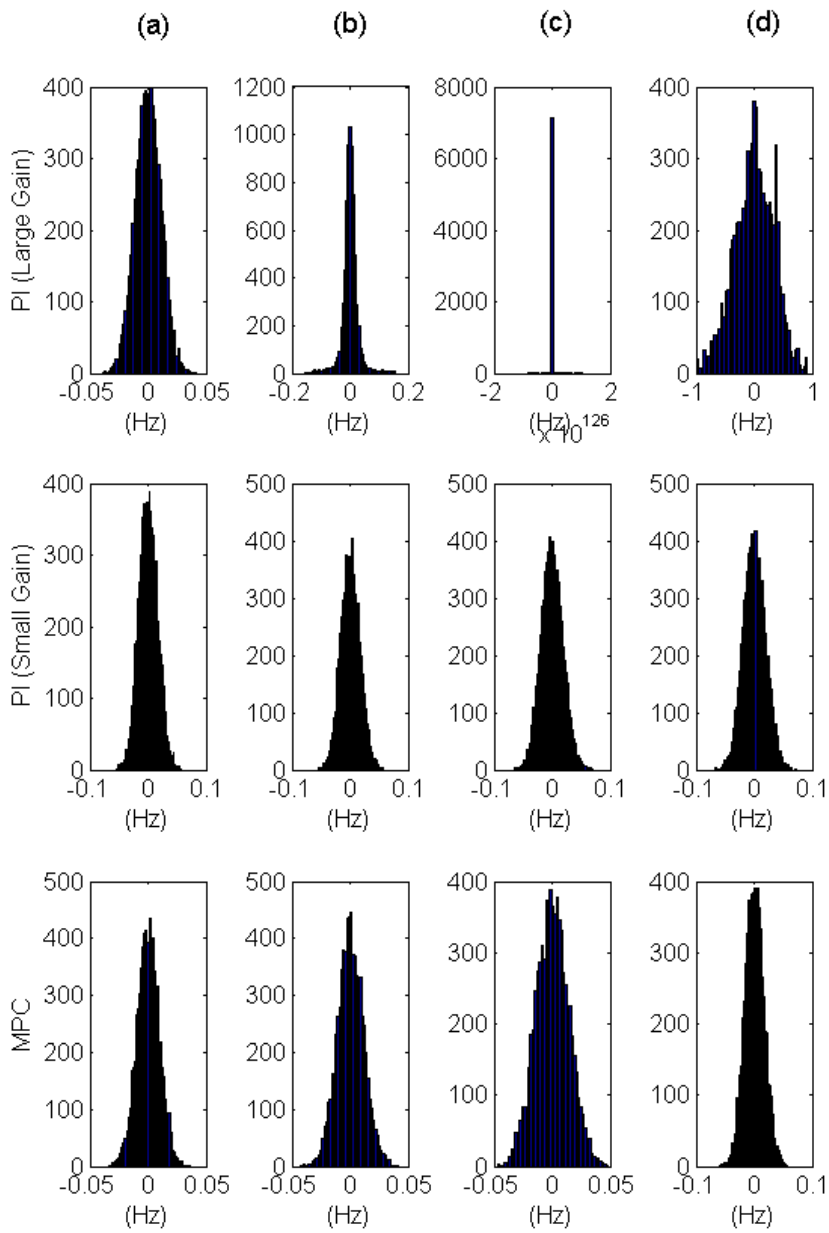

Figure 4. 7 Histograms of simulated data (frequency) in four scenarios in Gen2

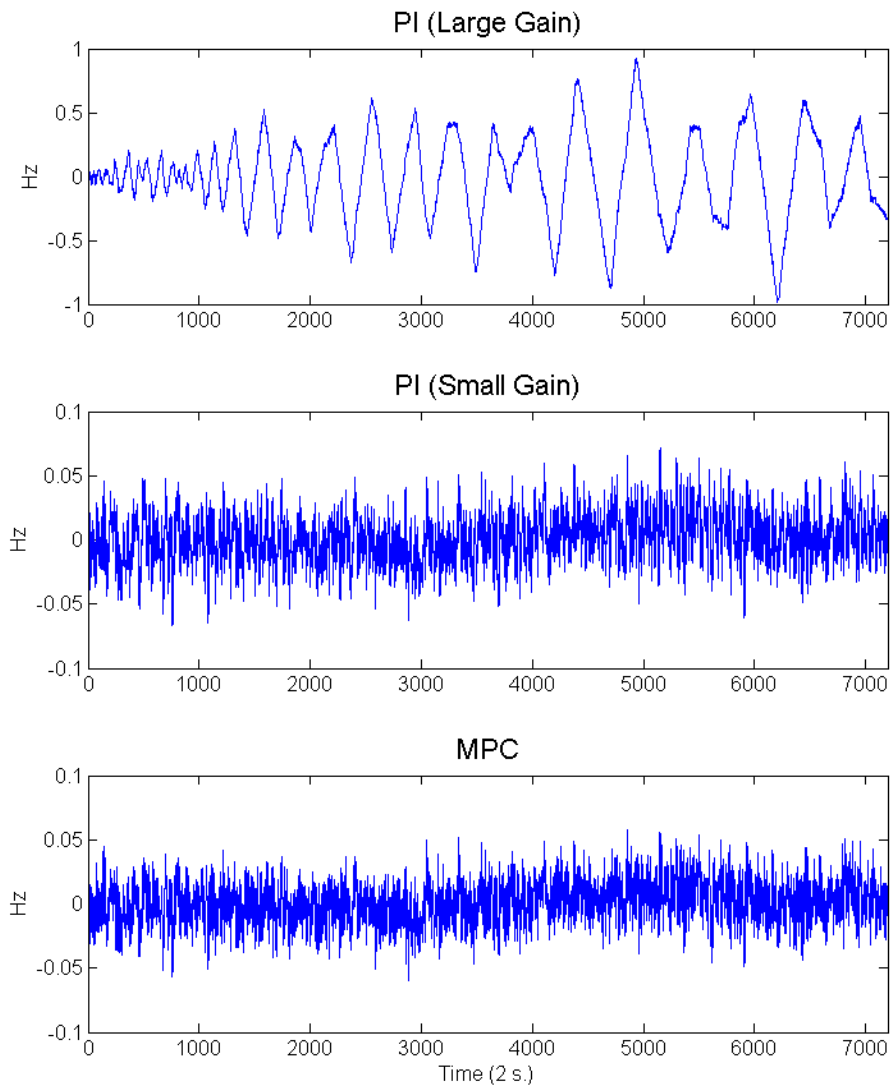

Figure 4. 8 Frequency results for constrained and delayed-input scenario for BA1

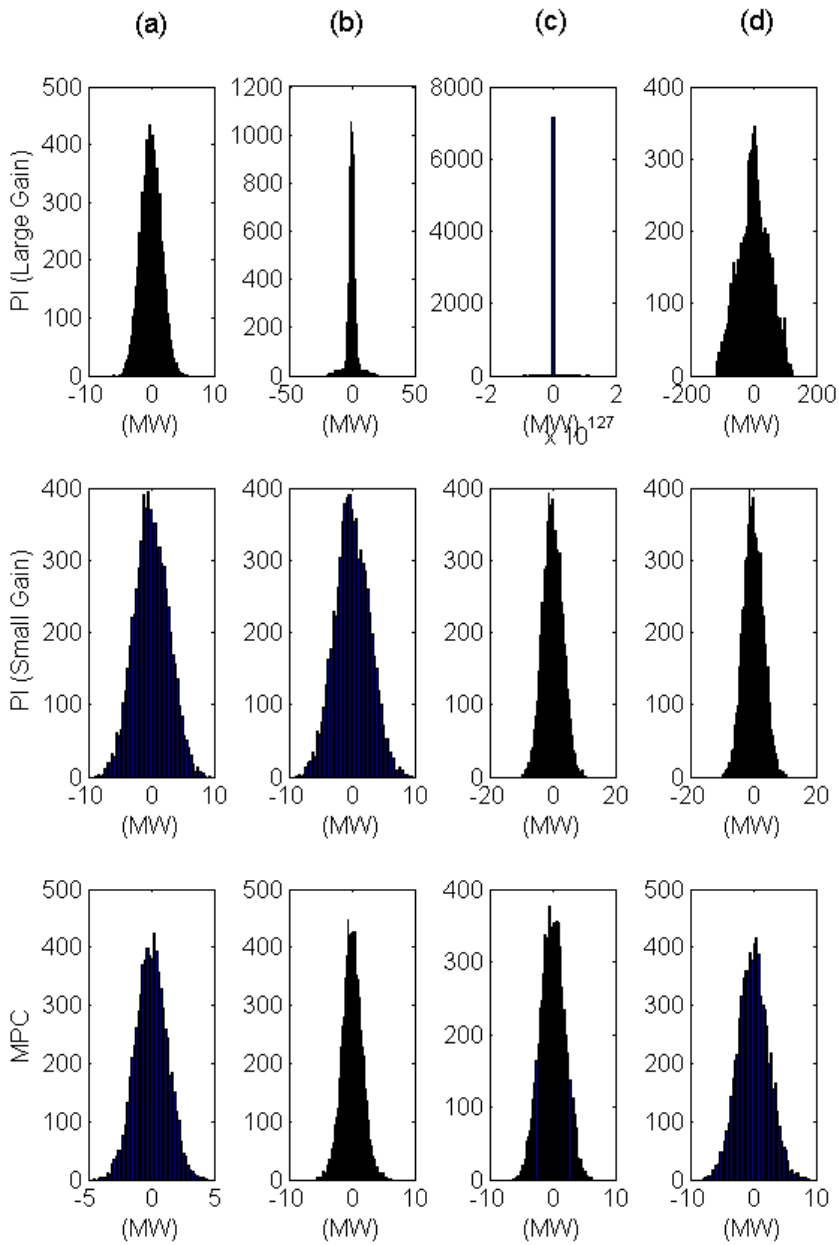

Figure 4. 9 Histograms of simulated data (ACE) in four scenarios in BA1

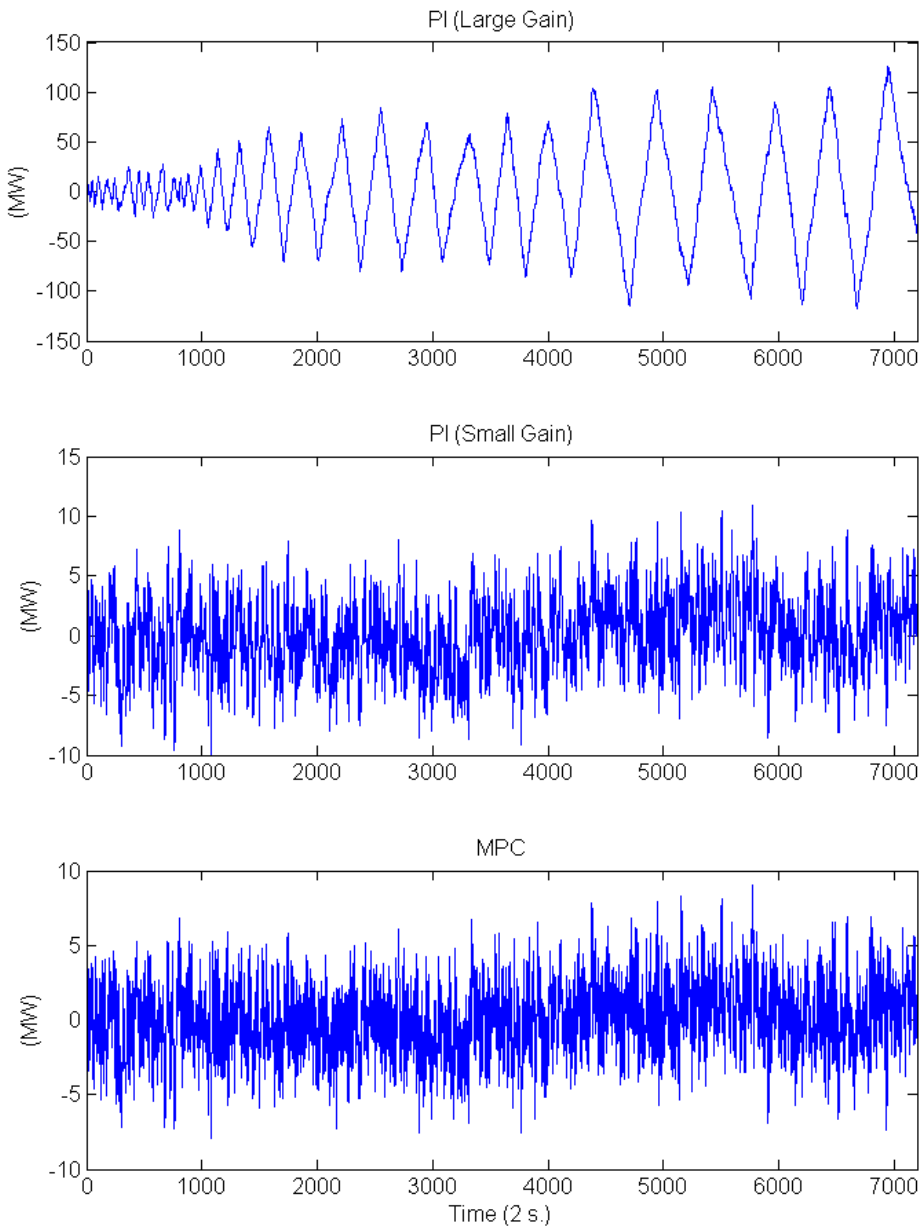

Figure 4. 10 ACE results for constrained and delayed-input scenario for BA1

4.2.2.2 CONTROL PERFORMANCE STANDARD RESULTS

In this section, we investigated CPS on each simulation case. For calculating CPS1 and CPS2, we set ϵ_1 to 0.0131 Hz, ϵ_2 to 0.0025 Hz [7, 38] and other parameters to Tables 4.3 and 4.4 in this paper. Specifically, we add an appendix for explanation of CPS[2].

The MPC-based approach conformed better to both CPS1 and CPS2 than the PI-based approaches. Figure 4.11 shows the CPS1 for BA 1 with four different scenarios of load reference constraints and input time delays. The results are similar to the results described in the previous section for a unit-step disturbance. Specifically, a large integral gain with the PI-based approach in Figure 4.7 provided conflicting results with delayed inputs. In the field, the degree of frequency deviations is very important in power system since mechanical devices such as steam turbine can be damanged and change the power angles among generators [1]. Therefore, the results in MPC-based approach are very helpful for the system operators who are in charge of stabilize the frequency.

In simulation, every control system failed to meet the system requirement of CPS1 when the generators were constrained and had delayed-inputs. In the field, the long-term mean μ is zero, and the power demands at each bus do not have a tendency such as continuously upward or downward demand since it can be offset via economic dispatch as another control process during system operation. However, the load model in this thesis was developed by Ornstein-Uhlenbeck process without considering long-run mean where the parameter θ in Table 4.7 is 0. Therefore, the load demands at each bus had a tendency such as continuously upward or downward demand (i.e. 250-360 s as shown in Figure 4.6). Therefore, the averaged 1-minute frequency and the averaged 1-minute ACE were significantly increased (or decreased) with such cases when the generators were constrained

[2] Appendix B

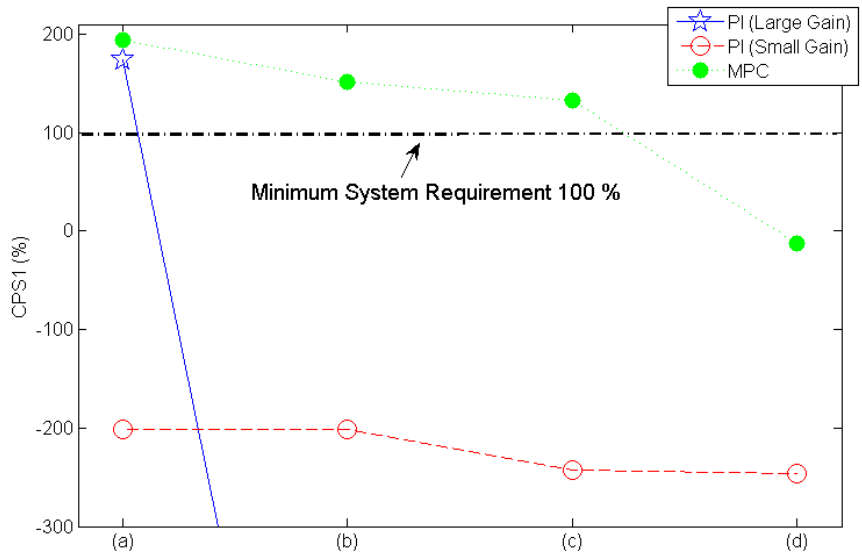

Figure 4. 11 CPS1 for BA1

and had delayed-inputs. Even though the proposed MPC-based approach did not satisfy the system requirement of CPS1, all results effectively showed that the proposed control had the dominant position as comparison with the PI-based control.

As a result of CPS2, the PI-based AGC with a large integral gain and delayed inputs provided poor results; however, the other scenarios or the other control systems conformed 100% which is over the minimum system requirement 90%. This situation signifies again that tuning of the integral gain in conventional PI-based approach is very important to secure good dynamic performance of stabilizing the frequency and maintaining the tie-line flows.

4.3 BULK-AREA PARTITIONING

4.3.1 SIMULATION SETTING

Simulation is conducted on a modified New England 39-bus system, as shown in Figure 4.12; per-unit bus voltage, bus angle, and transmission line data in Ref. [39, 40] are used. Table 4.8 lists the parameters and load reference constraints for the generator dynamic models at each bus. Table 4.9 lists the information of load disturbances.

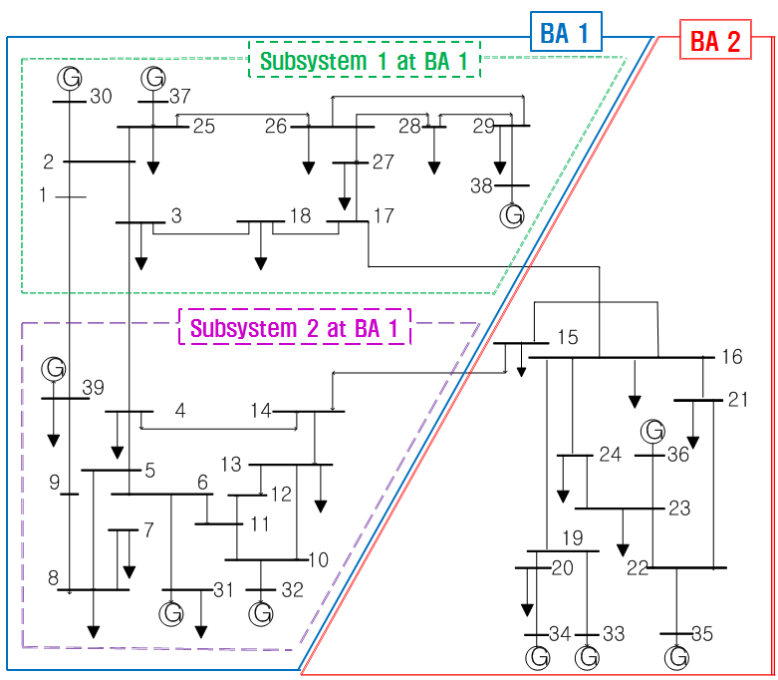

Figure 4. 12 IEEE 39 Bus systems with two BAs

This simulation demonstrates the results of both centralized (single-area case) and distributed MPC-based AGC (two-area case). The MPC-based operation results are analyzed from the perspectives of computational burden and dynamic performance.

Table 4. 9 Parameters for the 39-bus simulation in per unit

Generator Bus	M	D	T_g	T_a	K_t	r	$\bar{u}$ (10^{-4})	$\underline{u}$ (10^{-4})
# 30 (Gen1)	2	5	0.25	0.2	250	19	3	-3
# 31 (Gen2)	3	5	0.25	0.2	250	19	3	-3
# 32 (Gen3)	2	5	0.25	0.2	250	19	2	-2
# 33 (Gen4)	2	5	0.25	0.2	250	19	2	-2
# 34 (Gen5)	3	5	0.25	0.2	250	19	3	-3
# 35 (Gen6)	2	5	0.25	0.2	250	19	3	-3
# 36 (Gen7)	2	5	0.25	0.2	250	19	3	-3
# 37 (Gen8)	2	5	0.25	0.2	250	19	3	-3
# 38 (Gen9)	3	5	0.25	0.2	250	19	2	-2
# 39 (Gen10)	2	5	0.25	0.2	250	19	2	-2

Table 4. 10 Step load deviation events

Event time [s.]	Bus number	Magnitude [pu]
1	28	0.2
50	13	-0.1
100	22	0.15

4.3.2 SINGLE-AREA CASE

Table 4.11 lists the parameters for the MPC-based control simulation. Figure 4.13 shows that frequencies among generators are maintained by the given control scheme. We use a two-area notation rather than the original single-area notation to compare the distributed MPC-based results with the multi-area results.

Table 4. 11 Parameters for centralized MPC-based AGC

	Variable	Value
Discretized Minimum Step Time [s]	T_f	1
AGC Update Time [s]	T_u	2
Weighting Matrix	Q	$10^2 I$
	Q_N	$10^2 I$
	R	I
Prediction Horizon	N	20
Frequency Bias Factor	β	200

- I is a 10-by-10 identity matrix.

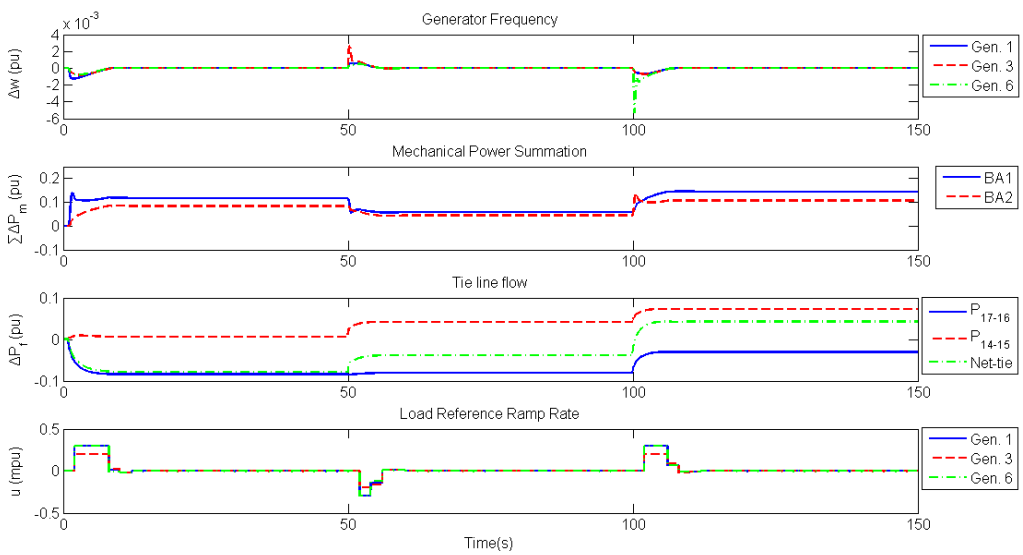

Figure 4. 13 Centralized MPC-based AGC (Single-area case)

In this simulation, the proposed controller provided very successful and satisfactory dynamic performance on stabilizing frequency, but the average time for the optimization of an MPC-based approach were much bigger in comparison to the distributed MPC-based results with the multi-area cases. The results show that each frequency at generator buses is rapidly maintained. Given that the centralized controller solves the optimization problem in consideration of the entire system dynamic behavior, its solution (load reference set-point control) usually provide better dynamic performance than the distributed MPC-based solution. However, as mentioned before, the computational complexity in this simulation was a greater problem since the number of optimization variables in MPC-based approach depends on the prediction horizon sizes and the system size. Specifically, the number of optimization variables in this case was 200 which was much bigger in comparison to distributed (partitioned)-area case.

4.3.3 MULTIPLE-AREA CASE

Tables 4.12 and 4.13 list the parameters for distributed MPC-based control simulation. All the conditions are assumed to be the same as in Table 4.11, except for frequency bias factors and system sizes at each BA. In case of bulk-area partitioning, BA1, as shown in Figure 4.12, has two subsystems with their own frequency controllers, and the mechanical power outputs in each subsystem are controlled by an upper controller in BA1 every 4 s.

In the bulk-area partitioning control scheme at Case 2, each subsystem in BA1 equally generates the discrepancy between the generation supply and the total MW obligation. In Figure 4.14 (Case1), although the mechanical power outputs among subsystems were different and did not become equal at Case1, the results at Case2 had the same mechanical power values in each subsystem. These results signified that each subsystem shared its power generation capacities. Moreover, Case3 and Case4 in Figure 4.14 showed the discriminative power sharing scheme in Equation (3.17), such a scheme should be cautiously considered in the future when renewable power sources and microgrids are briskly utilized in power system because these entities can produce large disturbances (P_L and F) to increase their profits.

Table 4. 12 Parameters for distributed MPC-based AGC for each BA

	Variable	BA 1	BA 2
Discretized Minimum Step Time [s]	T_f	1	1
AGC Update Time [s]	T_u	2	2
Weighting Matrix	Q	$10^2 I_1$	$10^2 I_2$
	Q_N	$10^2 I_1$	$10^2 I_2$
	R	I_1	I_2
Prediction Horizon	N	20	20
Frequency Bias Factor	β	120	80

- I_1 is a 6-by-6 identity matrix.

- I_2 is a 4-by-4 identity matrix.

Table 4. 13 Parameters for bulk-area partitioning in BA1

	Variable	SB1	SB2
participation rate	Case 1	Without partitioning	
	Case 2: α_k/n_i	1/2	1/2
	Case 3: α_k/n_i	0	1
	Case 4: α_k/n_i	1	0
Mechanical power sampling time [s]	T_m	4	
Weighting Matrix	Q	$10^2 I_{sb1}$	$10^2 I_{sb2}$
	Q_N	$10^2 I_{sb1}$	$10^2 I_{sb2}$
	R	I_{sb1}	I_{sb2}

-SB is subsystem.

-I_{sb1} and I_{sb2} are 3-by-3 identity matrices.

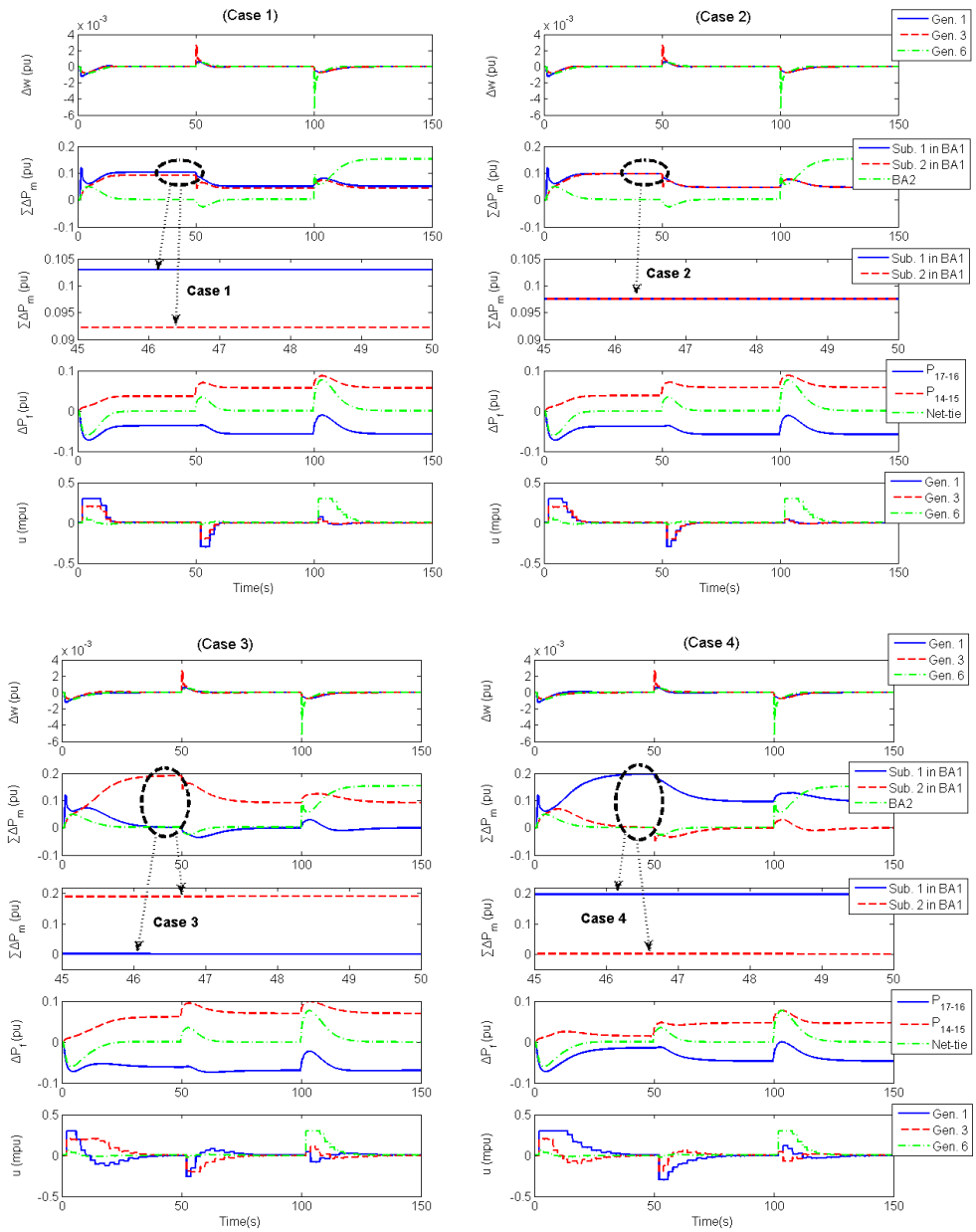

Figure 4. 14 Multi-Area Cases : (Case1) Without portioning; (Case2) With partitioning, each subsystem equally takes responsibility for balancing; (Case3) With partitioning, subsystem2 takes responsibility for balancing alone; (Case4) With partitioning, subsystem1 takes responsibility for balancing alone

Bulk-area partitioning dramatically reduces computation time and ensures dynamic performance. In this simulation, each subsystem has three generators, half of the original six generators in BA1. Therefore, the objective function in Equation (3.10) is much rapidly solved. In Figure 4.15, the results show the computation times in accordance with the horizon sizes and the number of states by using an Intel Core i5 CPU 750 @2.67 GHz and 2 GB of RAM. The prediction horizon size (N) affects the dynamic performance in stabilizing frequency and tie-line flows. Therefore, its size is manually chosen in accordance with the user-defined (or system) dynamic performance requirements. However, the number of generators is fixed and cannot be changed to a small value. In the MPC-based scheme, the numbers of generators in bulk areas will lead to computational burden, although simply modified SISO-based schemes, such as proportional–integral-based AGC, do not suffer greatly from this problem. The proposed bulk-area partitioning can mitigate this difficulty in solving a massive QP problem at a time by dividing the original state function. In addition, the results of the proposed scheme only present a slight difference in dynamic performance compared with the results in the (Case1) original case. This situation signifies that the bulk-area partitioning control scheme can provide substantial and realistic measures for suffering from "curse of dimensionality" as a desired result.

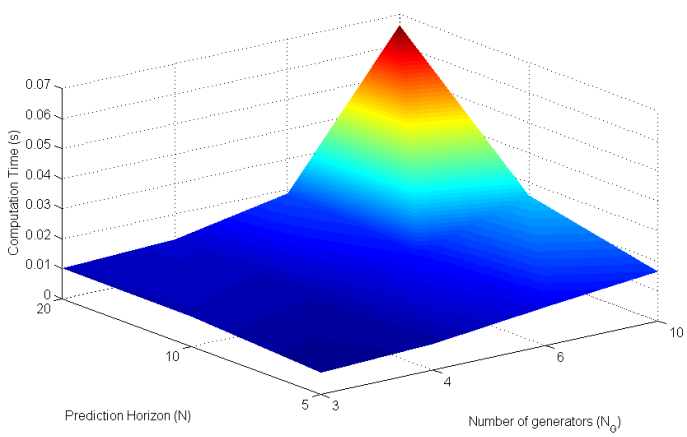

Figure 4. 15 Average computation times according to operation conditions

4.3.4 ANALYZING SYSTEM SIZE-DEPENDENT AGC SCHEME VIA MPC-BASED APPROACH

Based on the tested simulation results, structure-dependent MPC-based AGC can be considered, as shown in Table 4.14. Each scheme has unique advantages and disadvantages. Given that centralized control considers the entire system dynamic behavior, this scheme in the original case provides improved settling time results. However, centralized controllers in bulk-power systems have severe problems (Table 4.13). Therefore, under the control design process, system operators should cautiously analyze whether or not to satisfy the system requirements in designated MPC-based AGC structure.

Table 4. 14 Structure-dependent MPC-based AGC

	Centralized	Distributed Structure	
		Case1	Case2
Computation Time	X	Δ	O
Practicality	X	O	O
Settling time (T_{st}) [s]	7.60	13.31	13.91

* X : severe, Δ : less severe, O : least severe

* T_{st} : The maximum time required for every generator frequency curve to stay within a range of certain percentage 0. 01 % (0.1 mpu) of the nominal frequency from the first disturbance 0.2 pu at Bus28

Proposed structure-dependent MPC-based AGC schemes can help the system operators to prepare for future power systems. Due to increasing profit-seeking entities such as wind-farm producers and microgrid operators, sharing the responsibility of deviated system frequency (or power imbalance) among entities can be critical and will be very important issue in future. Based on proposed control structures, it is possible to consider how to share the responsibility of the deviated system frequency or to design the operation rules. For instance, system operator in a centralized structure should be responsible for stabilizing frequency by himself. However, he can reduce the computation burden as well as his

responsibility via the proposed bulk-area partitioning control scheme since owners (operators) in subsystems are required to build dispatchable power resources to meet the contraction like Eq. (3.17).

CHAPTER 5. CONCLUSIONS AND FUTURE WORKS

5.1 CONCLUSIONS

This thesis proposed an MPC-based approach for AGC to reduce the problems, such as decreasing the dynamic performances of AGC and control instability that results from the constraints of the load-reference set-point ramp rate and delayed inputs among generators. Given that power systems have various generators under different topologies, reflecting the characteristics of generators in the power networks and control system structures is necessary. Based on these considerations, we developed the MPC-based approach for AGC schemes in three different design processes.

First, we developed a tractable system model for time-delayed generator dynamics in power networks in which the input signals to the generators are delayed and constrained. Using the proposed MPC-based approach, we developed a conversion process for delayed-input system models to create an equivalent delay-free system model. Based on the obtained model, the proposed control system was not severely affected by handling constraints as well as delayed inputs among generators compared with the conventional PI-based approach. Specifically, when inputs are delayed among multiple generators, we showed that the future states (frequencies) should be considered on the basis of previous inputs (load-reference set point) because excessive control inputs without considering previous inputs result in control instability. The simulation results showed that the proposed MPC-based scheme provided the successful control results such as increasing the dynamic performance of AGC compared with the conventional PI-based approach.

Second, we developed a controller based on a quadratic cost criterion, which is a squared-weighted sum of states (wherein the regulated variables are the generator frequencies) and controls (i.e., load references) among multiple generators. A quadratic programming (QP)

algorithm was used to reduce the computational expense. This algorithm provided necessary and sufficient conditions for optimality because it was a convex optimization problem with differentiable objective and constraint functions, satisfying Slater's condition. Therefore, compared with the PI-based approach, the proposed controller could quickly compute and provide more accurate AGC signals. However, the controller had a computational burden caused by optimizing the objective function.

Finally, we developed a bulk-area partitioning scheme to reduce the computational cost. Given that a large number of generators may participate in AGC and the AGC signals should be computed rapidly (within approximately 2 s), we considered the computational costs of the MPC-based approach for AGC. Therefore, we first showed that the average times to compute the AGC signal increased according to the prediction horizon and the number of generators. Based on these results, we proposed a novel approach to divide the power system into multiple distributed subsystems to reduce the number of optimization variables. Specifically, this scheme mitigated the difficulty in solving a massive QP problem at a time by dividing the original optimization variables and computing AGC signals at each subsystem separately. In addition, the results of the proposed scheme only presented a slight difference in dynamic performance compared with the results of the method that did not partition the area.

The contributions of this study are summarized as follows:

First, this thesis showed the importance of developing the MIMO system controller to consider the future implications of current control action when inputs are delayed among multiple generators. Although the previous AGC studies via the PI-based approach showed that the delay significantly decreased the admissible controller gain and made the AGC system less stable, such research had a limitation in providing a fundamental solution to minimize the problems caused by multiple delayed inputs. Reflecting the generator

characteristics, such as multiple and different delayed inputs, is difficult when the PI-based approach is used.

Second, this thesis showed that shorter response times of generators are desirable to rapidly stabilize frequency deviations and inadvertent tie-line flows among BAs. This situation signifies that generators with a slow response time or under constrained conditions should be sublated when AGC signals are computed by the EMS in each BA. Additionally, battery energy storage system can be a valuable device for frequency regulation (AGC) because of its fast response characteristic.

Finally, this thesis showed that a centralized control structure has better control performance than distributed control structures. Given that the centralized controller solves the optimization problem in the entire system dynamic behavior, its solution (control signal) provides better dynamic performance than the distributed MPC-based solution. However, the centralized MPC-based AGC among independent bulk BAs can be considered as an impractical approach. Each BA should not only have its own AGC scheme, but optimizing AGC signals in a large-scale power system model also consumes considerable computational time to obtain an acceptable solution.

5.2 DIRECTION OF FUTURE WORKS

Adaptive Control Processes for Tuning Parameters

In practice, considering the system dynamics with uncertainties in a time-varying system is necessary to build a stable controller. In the field, obtaining complete information to describe the system matrix *A*, control matrix *B*, or other parameters such as the input delay *h* is impossible because of the additional unknown integral or external noise, environmental factors, and limited plant knowledge. Two different approaches to adoptive control theory have been widely adopted in the field. The first involves online learning approaches [41-43], which can aid the controller to accurately update and tune parameters. However, these approaches have significant limitations when large and unknown changes in the model parameters occur. Most robust approaches [44, 45] are based on stability considerations via a Lyapunov function method or linear inequality technique, which can aid in controller stabilization. The dynamic performance of the controller with the second of these approaches depends on the accuracy of the initial parameters and the level of uncertainty. We should develop both approaches in the field. Specifically, both approaches can also help the system operator to properly tune the integral gain in PI-based approaches to AGC.

Application Development of Information

We should consider the application of information in the MPC-based approach. In the field, the PI-based approach for AGC in each BA only minimizes ACE. Although it has information that includes the characteristics of multiple generators and the network model, it does not provide an effective method to use these data because it is a SISO-based scheme that does not consider the future implications of current control action. Specifically, when

inputs among multiple generators are delayed, the future states (frequencies) should be considered on the basis of previous inputs (load-reference set point) because excessive control inputs without considering previous inputs result in control instability. However, the MPC-based scheme described in this study is tractable and can consider multiple information to satisfy the system requirements and improve the dynamic performance of AGC. A major difference between the MPC-based and PI-based approaches is that system operators may select the essential information from the available data in the system based on the objective and constraints, as well as design the controller to satisfy the system requirements, such as stabilizing frequency and maintaining scheduled tie-line flows. This criterion should be considered when realizing an MPC-based approach, and is necessary to exploit the merits of the method and compare them with that of PI-based approaches.

Development of a Cost-based Resource Allocation Model with Performance-based Constraints

Most AGC studies mainly focused on satisfying the system requirements, such as control performance standard (CPS) and disturbance control standard (DCS). In addition, the settlement for frequency regulation is usually calculated according to the control results compared with the given AGC signal at each time. Therefore, determining and tuning the AGC participation rates based on operation costs including losses is important. However, tuning the participation rates based on the characteristics of such generators is difficult in the conventional PI-approach because the approach is a SISO-based control model. In the proposed controller, tuning the participation rates and considering the cost functions of the generator as well as developing the customized objective function, which is expected to help system operators reduce their operating costs, is more tractable.

Developing a Battery Energy Storage System Model for Frequency Regulation

In this thesis, we mainly showed the need to reflect the characteristics of generators in power networks to improve the dynamic performance of AGC. Recently, battery energy storage systems (BESS) have attracted attention because of their fast response characteristic. BESS should be modeled in the process design, and the controller for AGC should consider the characteristics of BESS, such as power-generation ramp rates and state of charge (SOC). Specifically, when the BESS owner/operator takes no SOC feedback control, the average SOC gradually decreases because of the energy conversion efficiency. Therefore, BESS should secure the dischargeable energy via SOC feedback control before energy shortage occurs. This study is expected to help system operators (or BESS owners) to stabilize the frequency by minimizing the operation cost of BESS or maximizing the profits from BESS.

APPENDIX

A. LINE FLOW CONTROL MODEL

This section provides the individual line flow control model in order to reduce the wheeling in the power network. As loop flows and arrangements for parallel path compensation become increasingly important, this developed control scheme supports system operators by reducing the increase in power losses or the overloading of network elements.

A.1 LINE FLOW CONTROL IN CENTRALIZED STRUCTURE [28]

In centralized control, the most attractive and distinguishing advantage is to control line flows because loop flows and arrangements for parallel path compensation become increasingly important as the demand for transmission capacity increases at a faster rate than actual capacity [46]. Therefore, we propose the control scheme to stabilize line flows in centralized MPC-based AGC.

From Equation (3.12), the state transition function for line flows can be described as follows:

$$\begin{aligned} P_f[k_{line}+1] &= P_f[k_{line}] + K_f(\delta_G[k_{line}+1] - \delta_G[k_{line}]) \\ &\quad + D_f(P_L[k_{line}+1] - P_L[k_{line}]) \\ &= P_f[k_{line}] + K_f T_{line} w_G^{set}[k_{line}] + D_f d[k_{line}], \\ &= A_f P_f[k_{line}] + B_f w_G^{set}[k_{line}] + D_f d[k_{line}] \end{aligned} \tag{A.1}$$

where k_{line} is the discretized line flow control time step. Load reference set-point signal w_G^{set} should be considered in Equation (A.1).

In a typical control design, the set-point command (path) is chosen as a smooth function that has no/few high-frequency components. Therefore, the time step k_{line} of w_G^{set} should be larger than the frequency control update time k_u and the state prediction time step k.

Optimal load reference set-point signal w_G^{set*} in the infinite horizon can be obtained from minimizing a criterion, such as:

$$J_\infty = \sum_{k=0}^{\infty} P_f[k_{line}+1]'\mathrm{Q}_f\, P_f[k_{line}+1] + w_G^{set}[k_{line}]'R_f\, w_G^{set}[k_{line}], \qquad \text{(A.2)}$$

From Equation (A.2), w_G^{set*} can be described as:

$$w_G^{set*}[k_{line}] = -K_G^{set} P_f[k_{line}], \qquad \text{(A.3)}$$

where:

$$K_G^{set} = (\mathrm{R} + \mathrm{B}_f^T PB_f)^{-1} \mathrm{B}_f^T PA_f\ , \qquad \text{(A.4)}$$

$$0 = A_f^T PA_f - P + Q_f - A_f^T P\mathrm{B}_f (\mathrm{R}_f + \mathrm{B}_f^T P\mathrm{B}_f)^{-1} \mathrm{B}_f^T PA_f\ , \qquad \text{(A.5)}$$

where P is the solution to the discrete algebraic Riccati equation [47, 48].

To drive the system to some other set-point w_G^{set}, w_k can be replaced with:

$$w_k^s = \omega_k - w_G^{set} \ , \tag{A.6}$$

The state transition function in Equation (3.1) can be expressed as:

$$\begin{aligned} w_{k+1}^s &= \mathrm{A}\left(\omega_k - w_G^{set}\right) + Bu_k - (I - A)w_G^{set} \\ &= \mathrm{A}w_k^s + Bu_k + \eta \end{aligned} \ , \tag{A.7}$$

where $\eta = -(I - A)\, w_G^{set}$.

On the basis of Equation (A.7), the predictive states for system frequency with a non-zero set-point w_G^{set} can be re-expressed as follows:

$$w_{k+i}^s = A^i w_k^s + \sum_{j=1}^{i} A^{i-j} B u_{k+j-1} + \sum_{j=1}^{i} A^{j-1} \eta \ , \tag{A.8}$$

$$W = M_w w_k^s + C_u U_k + D_s \eta \ , \tag{A.9}$$

where D_s is the $(N \times n) \times n$ matrix.

The attempt to minimize a squared-weighted sum of state (regulated variables) w and control u of the given Equation (A.8) is described by:

$$
\begin{aligned}
J_k &= \sum_{i=0}^{N-1}\left(\left\|w_{k+i|k}^{s}\right\|_{Q}^{2}+\left\|u_{k+i|k}\right\|_{R}^{2}\right)+\left\|w_{k+N|k}^{s}\right\|_{Q_N}^{2} \\
&= (M_w w_k^s + C_u U_k + D_s \eta)^T Q'(M_w w_k^s + C_u U_k + D_s \eta) \\
&\quad + U_k^T R' U_k + w_k^{s,T} Q w_k^s \\
&= U_k^T H U_k + 2(F_{w,1}^T U_k + F_{s,1}^T) U_k + c_1
\end{aligned}
\tag{A.9}
$$

where

$$F_{s,1} = C_u^T Q' D_s \ \eta;$$

c_1 is a constant.

In consideration of input constraints, the optimization of Equation (A.9) can be expressed as a quadratic program optimization:

$$
\begin{aligned}
&\min \ \frac{1}{2} U_k^T H U_k + \left(F_{w,1}^T + F_{S,1}^T\right) U_k \\
&\text{subject to} \\
&A_{in} U_k \le b_{in}
\end{aligned}
\tag{A.10}
$$

where A_{in} and b_{in} express the load reference ramp constraints among generators.

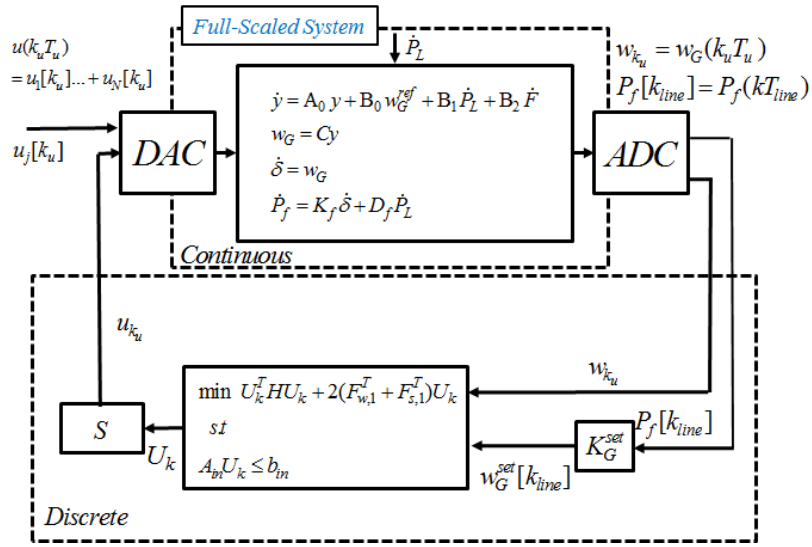

Figure A. 1 Centralized MPC-based AGC considering line-flows [28].

A.2 Simulation Results

This simulation demonstrates the results of centralized line flow control scheme in IEEE 39 bus system and uses Table A.1 and Table A.2 in the previous section. Table B.1 lists the parameters for the centralized MPC-based control simulation.

In this simulation, the proposed centralized controller maintains line flows P_{17-16} and P_{14-15}. Therefore, the 39-bus system naturally divides into two areas, BA1 and BA2 (Figure A.1). We use a two-area notation rather than the original single-area notation to compare the centralized MPC-based results with the distributed MPC-based results. As shown at Case 1 in Figure B.2, the individual lines were maintained.

In Figure B.1, each BA is responsible for its discrepancy between the generation supply and the total MW obligation through line flow control. This centralized controller adjusts the load references among generators to maintain the frequency every 2 s and to stabilize the inadvertent line flows every 6 s. The results show that BA1 and BA2 at 150 s produce

powers of 0.1 and 0.15 pu respectively as the load deviations in each BA. This line control scheme secures state controllability while the number of designated lines is fewer than the generators involved in the line flow control. In the simulation, the controllability in Equation (B.1) is satisfied because two line flows are controlled by 10 generators. On the basis of this control property, the system operator can design AGC to maintain frequency in consideration of designated and important line flows.

This line control scheme helps the system operator reduce wheeling, which is a loop flow caused by network topology. In the field, wheeling increases the power losses or the overloading of network elements. Therefore, wheeling must be considered to minimize operation cost and secure system reliability. However, most of the previous MPC-based schemes, which did not consider network topologies, could not provide any method to minimize the loop flows such as the results in Figure 4.12. Based on the proposed control scheme, designated lines were effectively adjusted as shown in Figure A.1, and it can help the system operators to reduce the power losses or the overloading of network elements.

Table A. 1 Parameters for centralized MPC-based AGC.

Description	**Parameter**	**Value**
Discretized Minimum Step Time [s]	T_f	1
AGC Update Time [s]	T_u	2
Line Control Update Time [s]	T_{line}	6
Weighting Matrix	Q	$10^2 I$
	Q_N	$10^2 I$
	R	I
	Q_f	I_{line}
	R_f	I
Prediction Horizon	N	20
Frequency Bias Factor	β	200

- I is a 10-by-10 identity matrix. - I_{line} is a 2-by-2 identity matrix.

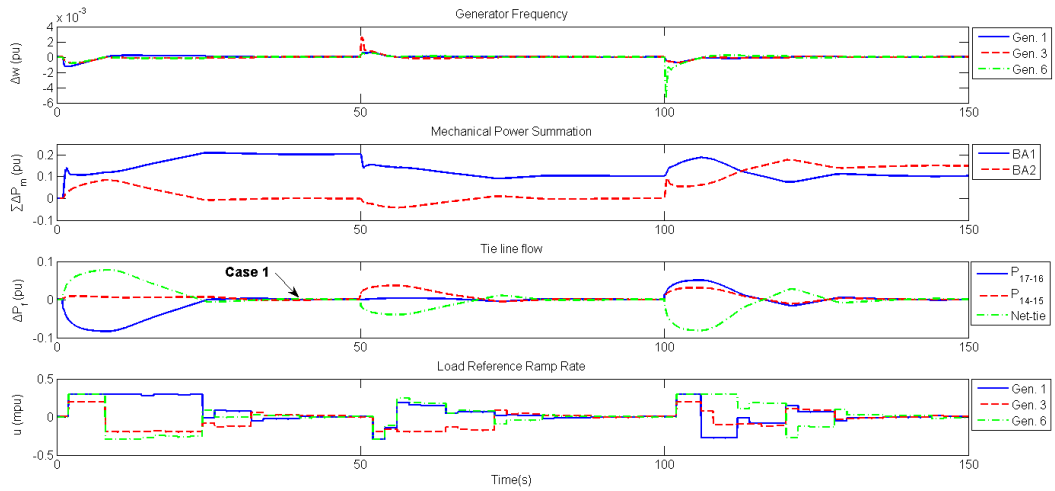

Figure A. 2 Centralized MPC-based AGC with the proposed line flow control

B. CONTROL PERFORMANCE STANDARD (CPS)

Control Performance Standards CPS1 and CPS2 were enacted by NERC in 1997 to evaluate a balancing area's frequency control performance in normal interconnected power system operations [38]. These criteria, or standards, assess characteristics of an area's "area control error (ACE)". Specifically, the motivation underlying CPS is to ensure a targeted long term frequency control performance of the entire interconnection [49], which is usually based on an interconnection's historical frequency profile. Therefore, the results of CPS indicates whether an area's generation is adequately controlled to make interchange meet its schedule and interconnection frequency support obligation [3], [10].

B.1. CPS1

CPSl is a limit on the average of a function combining *ACE* and interconnection frequency error from schedule. Specifically, it indicates the long term (12 month) frequency performance in the interconnection by measuring each balancing area's contribution to it

[38, 50]. The targeted control objective underlying CPS1 is to bound excursions of 1-minute average frequency error, Δf_{1min}, which is given as follows, over 12 months in the interconnection.

$$\Delta f_{1\min} = \frac{1}{M}\sum_{i=1}^{M}(f_i - f_0), \tag{A.1}$$

where is f_i the sampled actual system frequency and M is the number of actual system frequency samples in 1 minute.

As the interconnection frequency error is proportional to the sum of all balancing areas' *ACE*s, maintaining averages of *ACE*s within proper bounds will maintain the corresponding averages of frequency error within related bounds. With the interconnection frequency control responsibilities being distributed among balancing areas, CPS1 measures control performance by comparing how well a balancing area's *ACE* performs in conjunction with the frequency error of the interconnection. It is given by

$$CPS1 = (2 - CF)\times 100\%, \tag{A.2}$$

$$CF = \frac{(CF_{1\min})_{12month}}{(\varepsilon_1)^2}, \tag{A.3}$$

$$CF_{1\min} = \left[\left(\frac{ACE}{-10\mathrm{B}}\right)_{1\min}\times \Delta f_{1\min}\right], \tag{A.4}$$

Here, *CF* is the compliance factor, the ratio of the 12 month average control parameter CF_{1min} divided by the square of the frequency target ε_1. ε_1 is the maximum acceptable steady-state frequency deviation; it is 0.018Hz in the EI, 0.0228Hz in the Western

Interconnection (WI) and 0.020Hz for ERCOT [49]. It is developed from analysis of historical frequency data of each interconnection (which results in different targets for each of the interconnections). NERC monitors each interconnection's frequency performance and can tighten (or loosen) the ε_1 values should an interconnection's frequency performance decline (improve) [50]. The control parameter CF_{1min} is the 1-minute control unit for each balancing area in achieving the control objective. It indicates the extent to which the balancing area is contributing to or hindering correction of the interconnection frequency error. If the sign of CF_{1min} is negative, then the balancing area is contributing to the needed frequency correction. If positive, the balancing area is hindering the needed frequency correction. *B* is the frequency bias term in the *ACE* equation.

The minimum score of CPS1 compliance is 100%. If an area has a compliance of 100%, it is providing exactly the amount of frequency support required. Anything above 100% is considered "helping" interconnection frequency whereas anything below 100% is considered "hurting" interconnection frequency.

B.2. CPS2

CPS2 is a measure of a balancing area's *ACE* over all 10-minute periods in a month. The control objective is to bound unscheduled power flows between balancing areas. It was put in place to address the concern that a balancing area could improve its CPS1 by grossly over- or under-generating to obtain a large ACE (as long as it was opposite the frequency error) ; yet the large ACE would necessarily result in excessive flow deviations on the connections with neighbors. It is given by

$$CPS2 = 100(1 - \frac{Num\left(\left|(ACE)_{10\min}\right| \geq L_{10}\right)}{Num\left(all\ \left|(ACE)_{10\min}\right|\ \right)})\%\ , \qquad \text{(A.5)}$$

where $(ACE)_{10min}$ is the 10-minute average of the balancing area's *ACE*, Num(·) denotes the number of $|(\mathrm{ACE})_{10min}|$ that satisfies $|(\mathrm{ACE})_{10min}| \geq \mathrm{L}_{10}$ in one month, and

$$L_{10} = 1.65\varepsilon_2\sqrt{(10B_i)(10B_s)}\,, \tag{A.2}$$

L_{10} in MW describes the maximum value within which 10-minute *ACE* should be controlled. It is computed with the targeted 10-minute average frequency error bound for the interconnection ε_2, frequency bias of the balancing area, B_i, and the sum of all B_i'*s* (including the balancing area for which CPS2 is being computed) in the interconnection, B_s. ε_2 is developed from historical frequency data of each interconnection; it is 0.0057 Hz for EI and 0.0073 for the WI and ERCOT [49]. In 2003, the $10B_s$ were about -5692 MW/0.1Hz for the EI, -1825 MW/0.1Hz for the WI, and -920 MW/0.1Hz for ERCOT [49]. The minimum acceptable CPS2 score for each balancing area is 90%.

BIBLIOGRPHY

[1] "EPRI Power System Dynamics Tutorial," Electric Power Research Institute 1016042, Jul. 2009.

[2] R. Dunlop and D. Ewart, "System requirements for dynamic performance and response of generating units," *Power Apparatus and Systems, IEEE Transactions on,* vol. 94, pp. 838-849, 1975.

[3] C. Concordia, F. DeMello, L. Kirchmayer, and R. Schultz, "Effect of prime mover response and governing characteristics on system dynamic performance," in *Proceeding American Power Conference*, 1966.

[4] S. Ayasun and C. O. Nwankpa, "Stability of a two-area automatic generation control system with communication delays," in *Electrical and Electronics Engineering, 2009. ELECO 2009. International Conference on*, 2009, pp. I-65-I-69.

[5] L. Jiang, W. Yao, Q. Wu, J. Wen, and S. Cheng, "Delay-dependent stability for load frequency control with constant and time-varying delays," *Power Systems, IEEE Transactions on,* vol. 27, pp. 932-941, 2012.

[6] S. Bhowmik, K. Tomsovic, and A. Bose, "Communication models for third party load frequency control," *Power Systems, IEEE Transactions on,* vol. 19, pp. 543-548, 2004.

[7] T. Sasaki and K. Enomoto, "Dynamic analysis of generation control performance standards," *Power Systems, IEEE Transactions on,* vol. 17, pp. 806-811, 2002.

[8] H. Bevrani and T. Hiyama, "Robust decentralised PI based LFC design for time delay power systems," *Energy Conversion and Management,* vol. 49, pp. 193-204, 2008.

[9] H. Bevrani, *Robust power system frequency control* vol. 85: Springer, 2009.

[10] X. Z. Liu, "Structural modeling and hierarchical control of large-scale electric power systems," Dissertation, Massachusetts Institute of Technology, 1994.

[11] D. B. Eidson, "Estimation and hierarchical control of market-driven electric power systems," Dissertation, Massachusetts Institute of Technology, 1995.

[12] M. D. Ilic and J. Zaborszky, *Dynamics and control of large electric power systems*: Wiley New York, 2000.

[13] U. OpHB-Team, "UCTE Operation Handbook Appendix 1: Load-Frequency Control and Performance," 2004.

[14] P. Kundur, N. J. Balu, and M. G. Lauby, *Power system stability and control* vol. 7: McGraw-hill New York, 1994.

[15] K. J. Aström and T. Hägglund, "PID controllers: theory, design and tuning," 1995.

[16] A. Visioli, *Practical PID control*: Springer Science & Business Media, 2006.

[17] H.-S. Park and K.-J. Kim, "A study on AGC scheme based on real time frequency characteristics," in *Universities Power Engineering Conference, 2008. UPEC 2008. 43rd International*, 2008, pp. 1-5.

[18] H.-S. Park, "AGC algorithm based on real time frequency characteristics," Dissertation, Chungnam National University, 2009.

[19] E. F. Camacho and C. B. Alba, *Model predictive control*: Springer Science & Business Media, 2013.

[20] T. Mohamed, H. Bevrani, A. Hassan, and T. Hiyama, "Model predictive based load frequency control design," in *16th International Conference of Electrical Engineering, Busan, Korea*, 2010.

[21] L. Kong and L. Xiao, "A new model predictive control scheme-based load-frequency control," in *Control and Automation, 2007. ICCA 2007. IEEE International Conference on*, 2007, pp. 2514-2518.

[22] A. M. Yousef, "Model predictive control approach based load frequency controller," *WSEAS Transactions on Systems and Control,* vol. 6, pp. 265-275, 2011.

[23] E. Camponogara, D. Jia, B. H. Krogh, and S. Talukdar, "Distributed model predictive control," *Control Systems, IEEE,* vol. 22, pp. 44-52, 2002.

[24] A. N. Venkat, I. A. Hiskens, J. B. Rawlings, and S. J. Wright, "Distributed MPC strategies with application to power system automatic generation control," *Control Systems Technology, IEEE Transactions on,* vol. 16, pp. 1192-1206, 2008.

[25] H. Nong and X. Liu, "Nonlinear distributed MPC strategy with application to AGC of interconnected power system," in *Control and Decision Conference (CCDC), 2013 25th Chinese*, 2013, pp. 3935-3940.

[26] M. Ma, H. Chen, X. Liu, and F. Allgöwer, "Distributed model predictive load frequency control of multi-area interconnected power system," *International Journal of Electrical Power & Energy Systems,* vol. 62, pp. 289-298, 2014.

[27] T. Mohamed, H. Bevrani, A. Hassan, and T. Hiyama, "Decentralized model predictive based load frequency control in an interconnected power system," *Energy Conversion and Management,* vol. 52, pp. 1208-1214, 2011.

[28] Y.-S. Jang, J. Park, and Y. T. Yoon, "Designing Structure-Dependent MPC-Based AGC Schemes Considering Network Topology," *Energies,* vol. 8, pp. 3437-3454, 2015.

[29] Y. V. Makarov, S. Lu, J. Ma, T. B. Nguyen, and C. E. Commission, *Assessing the value of regulation resources based on their time response characteristics*: Pacific Northwest National Laboratory, 2008.

[30] M. Sipser, *Introduction to the Theory of Computation*: Cengage Learning, 2012.

[31] D. Axehill, "Integer quadratic programming for control and communication," Dissertation, Dept. Elect. Eng, Linköping University, 2008.

[32] P. TøNdel, T. A. Johansen, and A. Bemporad, "An algorithm for multi-parametric quadratic programming and explicit MPC solutions," *Automatica,* vol. 39, pp. 489-497, 2003.

[33] L. C. Saikia, S. Mishra, N. Sinha, and J. Nanda, "Automatic generation control of a multi area hydrothermal system using reinforced learning neural network controller," *International Journal of Electrical Power & Energy Systems,* vol. 33, pp. 1101-1108, 2011.

[34] S. Ghoshal, "Optimizations of PID gains by particle swarm optimizations in fuzzy based automatic generation control," *Electric Power Systems Research,* vol. 72, pp. 203-212, 2004.

[35] H. Zeynelgil, A. Demiroren, and N. Sengor, "The application of ANN technique to automatic generation control for multi-area power system," *International journal of electrical power & energy systems,* vol. 24, pp. 345-354, 2002.

[36] G. A. Chown and R. C. Hartman, "Design and experience with a fuzzy logic controller for automatic generation control (AGC)," *Power Systems, IEEE Transactions on,* vol. 13, pp. 965-970, 1998.

[37] S. Boyd and L. Vandenberghe, *Convex optimization*: Cambridge university press, 2004.

[38] N. Jaleeli and L. S. VanSlyck, "NERC's new control performance standards," *Power Systems, IEEE Transactions on,* vol. 14, pp. 1092-1099, 1999.

[39] M. Pai, *Energy function analysis for power system stability*: Springer Science & Business Media, 1989.

[40] R. D. Zimmerman and C. E. Murillo-Sánchez, "MATPOWER 5.0.0 User's Manual," *Power Systems Engineering Research Center, Cornell University, Ithaca, NY,* 2014.

[41] C. Venkateswarlu and K. V. Rao, "Dynamic recurrent radial basis function network model predictive control of unstable nonlinear processes," *Chemical engineering science,* vol. 60, pp. 6718-6732, 2005.

[42] C.-H. Lu, "Design and application of stable predictive controller using recurrent wavelet neural networks," *Industrial Electronics, IEEE Transactions on,* vol. 56, pp. 3733-3742, 2009.

[43] Y. Pan and J. Wang, "Model predictive control of unknown nonlinear dynamical systems based on recurrent neural networks," *Industrial Electronics, IEEE Transactions on,* vol. 59, pp. 3089-3101, 2012.

[44] Y. S. Moon, P. Park, and W. H. Kwon, "Robust stabilization of uncertain input-delayed systems using reduction method," *Automatica,* vol. 37, pp. 307-312, 2001.

[45] D. Yue and Q.-L. Han, "Delayed feedback control of uncertain systems with time-varying input delay," *Automatica,* vol. 41, pp. 233-240, 2005.

[46] A. J. Wood and B. F. Wollenberg, *Power generation, operation, and control*: John Wiley & Sons, 2012.

[47] C. L. Phillips and H. T. Nagle, *Digital control system analysis and design*: Prentice Hall Press, 2007.

[48] D. P. Bertsekas, *Dynamic programming and optimal control* vol. 1: Athena Scientific Belmont, MA, 1995.

[49] N. Jaleeli and L. VanSlyck, "Control performance standards and procedures for interconnected operation," *Electric Power Research Institute Report TR-107813, June,* vol. 10, 1997.

[50] C. Wang and J. D. McCalley, "Impact of wind power on control performance standards," *International Journal of Electrical Power & Energy Systems,* vol. 47, pp. 225-234, 2013.

논문 초록

본 논문은 전력시스템에서 기존의 비례적분제어(Proportional Integral: PI) 기반의 자동발전제어 (Automatic Generation Control: AGC) 설계시스템이 발전기의 부하 기준 설정에 대한 제약 (load reference set-point constraints) 및 시지연 (delayed inputs)으로 생기는 제어 성능 저하와 제어 불안정성에 대한 문제점들을 줄이고자 모델예측제어(Model Predictive Control: MPC) 기반의 자동발전제어 설계방안을 연구하였다. 일반적으로, 기존의 비례적분제어 기법의 제어기 설계는 단일 입력 단일 출력 (Single Input Single Output) 형태이므로 상기의 문제들에 대해 다루는데 어려움이 있으며, 계통이 커지고 발전기의 수가 많아짐에 따라서 그 어려움은 점점 커지게 된다. 위 고려사항을 바탕으로 본 논문은 모델예측제어기반의 자동발전제어 설계 방안에 대해 다음과 같이 개발하였다.

첫 번째로, 본 논문은 연속 시간 네트워크-발전기 모델에서 발전기들의 특성을 고려한 이산 제어기 설계 공정을 개발하게 된다. 본 논문에서 사용하게 된 연속 시간 네트워크-발전기 모델은 Massachusetts Institute of Technology 에서 연구 개발된 사항으로 네트워크 상에서 다수의 발전기들을 표현한 동적 시스템 모델이다. 이는 실제 시스템에서와 같이, 네트워크 상에 발전기들이 같은 제어지역에 있더라도 서로 다른 주파수를 가질 수 있다는 것을 표현해 준다. 즉, 기존 지역통제오차 (Area Control Error) 계산시에 사용되는 시스템 주파수는 해당 지역을 대표하는 주파수를 의미한다. 실제 시스템에서 자동발전제어 신호는

일정한 시간간격으로 발전기들에게 전달되므로, 본 논문은 위 연속 시간 네트워크-발전기 모델로부터 이산 제어기를 구현하기 위해 다양한 시간의 척도들을 활용함과 동시에 발전기들을 제어하기 위한 설계 공정에 대한 연구를 진행하였다.

두 번째로, 모델예측제어기법을 사용한 본 논문은 발전기들의 시지연 모델을 시지연을 가지지 않는 모델로 변경하는 전환 과정(conversion process) 개발 및 변경된 모델을 바탕으로 제어기를 개발하게 된다. 제안되는 전환 과정을 통해서 기존 PI 제어기가 시지연 시스템에서 문제를 가질 수 밖에 없는 요인에 대해서 분석을 하게 되며, 전환되어 얻어진 모델로부터 발전기특성을 고려한 제어기를 설계하게 된다. 이때 제어기는 주파수와 부하설정기준 제어 신호에 대한 가중합을 최소화하는 목적함수를 가지도록 설계함으로써, 본 논문은 해당 제어기의 목적함수를 이차 계획법 (Quadratic programming)의 문제로 변경하여 최적해 (자동발전제어 신호) 도출시간을 줄일 수 있도록 하였다.

마지막으로, 본 연구는 계산시간을 줄이기 위해 시스템 분할 기법을 제안하게 된다. 제안되는 제어기는 큰 규모의 시스템상에 존재하는 많은 수의 발전기들에 의해 자동발전제어 신호 계산에 부담을 가지게 된다. 이는 기존 단일 입력 단일 출력 형태의 비례적분제어기반의 시스템에서는 크게 영향을 받지 않은 문제이다. 따라서 본 논문은 발전기의 수 증가에 따른 계산시간에 대해 비교하며,

자동발전제어의 목적을 충족시키면서 계산시간을 효과적으로 줄이기 위한 시스템 분할 기법에 대해서 새롭게 제안한다.

시뮬레에션에서는 기존의 비례적분제어기법과 제안되는 모델예측제어기법에 대해서 비교 분석하게 된다. 우선 본 논문은 발전기의 부하 기준 설정 대한 제약 및 시지연에 대한 고려를 바탕으로 네 가지의 시나리오 결과를 도출하게 된다. 그리고 도출된 결과는 주파수가 안정화되는데 걸리는 시간, 지역 연계선로 상에 의도치 않게 흐른 전력량, 그리고 북미의 제어 성능평가 지수 CPS 를 바탕으로 비교 분석하게 된다. 추가적으로, 해당 제어기에 대한 계산시간 분석을 하게 된다.

주요어:

자동발전제어, 모델예측제어, 다중입출력 시스템, 전력네트워크, 시지연 시스템

학 번: 2009-20885